الجمهورية الجزائرية الديمقراطية الشعبية
People's Democratic Republic of Algeria
وزارة التعليم العالي والبحث العلمي
Ministry of Higher Education and Scientific Research

Mohamed Khider University - Biskra
Faculty of Science and Technology
Department: Civil and Hydraulic Engineering
Ref: ……

جـــامعة محمد خـيـضر بـــسكرة
كـلية الـعلـــوم و التكـــنولوجـيا
قسم : الهنـدسـة المـدنيـة و الـري
المـرجع : .....

MASTER END OF STUDY

Field: Civil Engineering

Specialty: Geotechnical

Behavior and design of back-to-back mechanically stabilized earth walls

---

Presented by:

BAALI Lamis

Supervisor:

Dr. DRAM Abdelkader

Academic Year: 2021-2022.

ACKNOWLEDGEMENTS

First and foremost, I wish to give all the praise to Almighty Allah for giving me the strength and time to complete this research.

I would like to sincerely thank Dr. Dram Abdelkader from the University of Biskra, my supervisor and thesis director for providing the scientific supervision of this thesis. I must admit that he knew well, first during the work of my master's thesis, and then during this thesis, to point me in the right way in times of confusion. His availability, his experience, and his thoroughness allowed this thesis to succeed. It was also a great pleasure for me to work under his direction.

Finally, I would like to express my deepest gratitude to my father, my mother, my brother, my sisters for their unflinching support, encouragement and love. Without them, this would not have been possible. Special thanks are reserved for those who encouraged me to complete this thesis.

Abstract

This thesis presents a literature search for geosynthetics reinforcement in back-to-back walls, and on the other, it analyzes the characteristics that lead to a conservative study. The goal of this thesis is to contribute to the understanding of the behavior of geogrid reinforced soil BBMSE walls by numerically analyzing the tensile loads in the geogrids, as well as the lateral earth pressure and lateral facing displacements. For a better understanding of the behavior of geosynthetics reinforced soil back-to-back mechanically stabilized earth (MSE) walls, a number of geometric and mechanical characteristics have been examined and implemented in the numerical code Plaxis 2D.

Keywords: Retaining walls, Geosynthetics, Reinforced soil, Numerical Modelling.

ملخص

قدم هذه الأطروحة بحثًا أدبيًا عن تقوية طبقات الأرض الاصطناعية في الجدران من الخلف إلى الخلف، ومن ناحية أخرى، تحلل الخصائص التي تؤدي إلى دراسة متحفظة. الهدف من هذه الأطروحة هو المساهمة في فهم سلوك جدران BBMSE للتربة المعززة بشبكة الجيوسنتتك من خلال التحليل العددي لأحمال الشد في طبقات الجيوسنتتك، بالإضافة إلى ضغط الأرض الجانبي وحالات النزوح الجانبية المواجهة. من أجل فهم أفضل لسلوك التربة الاصطناعية المعززة للجدران الأرضية المستقرة ميكانيكيًا (MSE)، تم فحص عدد من الخصائص الهندسية والميكانيكية وتنفيذها في الكود العدديPlaxis2D .

كلمات مفتاحية: **النمذجة الرقمية، جوستتيك، تربة مدعمة، جدران الاستناد.**

CONTENTS

LIST OF ABBREVIATIONS

LIST OF FIGURES

LIST OF TABLES

First Part: Literature Review

Chapter 1

Reinforced soil of mechanically stabilized earth walls

Chapter 2

Analysis of geosynthetic-reinforced soil retaining walls

Second Part: Numerical Modeling

Chapter 3

Analysis of Back-to-Back Reinforced Retaining Walls with Panel Facia

LIST OF ABBREVIATIONS

a	acceleration
g	acceleration due to gravity
f_{max}	maximum frequency of the seismic input motion
f	frequency of the seismic input motion
f_n	natural frequency of soil mass
λ_{min}	wavelength of shear wave
α, β	Rayleigh damping parameters
K	stiffness matrix of the system
M	mass matrix of the system
F_h	horizontal inertial force
F_v	vertical inertial force
H	height of the retaining wall
h	application point locations of the dynamic thrust
Δx	lateral displacement of the stem
z	height of the stem
t	thickness of tire shreds cushion
γ	unit weight of the soil
E	Young's modulus
φ	friction angle of backfill
ψ	dilatancy angle
δ'	interface friction angle
c	cohesion
v	Poisson's ratio
v_s	shear wave velocity
R_{inter}	interface strength-reduction factor
EA	elastic stiffness
EI	flexural rigidity
θ	rotation of the stem
N^*	normalized shear force

M^*	normalized bending moment
σ^*_E	normalized seismic earth pressure
σ_h	effective vertical pressure
σ_v	effective lateral confining pressure
P_{stem}	seismic earth pressure thrust at the stem
P_{heel}	seismic earth pressure thrust at the vertical section the heel
L	reinforcement length
D	distance between two opposing walls
$Tmax$	maximum tensile force in each reinforcement
S_H	horizontal spacing between reinforcement
S_V	vertical spacing between reinforcement
K_A	earth pressure coefficient
P_A	static active earth pressure
K_{AE}	total (static and dynamic) earth pressure coefficient
ΔK_{AE}	incremental dynamic earth pressure coefficient
P_{AE}	total thrust (static and dynamic)
ΔP_{AE}	incremental dynamic earth thrust
M-O	Mononobe-Okabe
S-W	Seed and Whitman
2D	two-dimensional
LVDT	linear variable displacement transformers
STD	scraps tire-derived
TDA	Tire Derived Aggregate
STC	sand–tire chips
EPS	expanded polystyrene
BBMSE	Bak-to-back mechanically stabilized earth
FHWA	Federal Highway Administration

LIST OF FIGURES

Chapter 1

Reinforced soil of mechanically stabilized earth walls

Chapter 2

Analysis of geosynthetic-reinforced soilretaining walls

Chapter 3

Analysis of Back-to-Back Reinforced Retaining Walls with Panel Facia

LIST OF TABLES

GENERAL INTRODUCTION

Reinforced soil retaining walls have been increasingly popular around the world, including in Algeria, in recent decades. These constructions are particularly popular due to their cost-effectiveness, architectural advantages over traditional retaining walls, and stable behavior. The interposition of reinforcement elements, specifically geotextile layers, in an earth structure is one of the ways to give the soils that make up the structure a certain tensile strength. As a result, geotextile reinforcement solutions can allow for the use of high-quality backfill materials while also being cost-effective. The behavior of load-bearing abutments and double-shell walls in geosynthetic reinforced soil is very complex. geosynthetic reinforced soil is very complex, it involves some important factors such as the geometric geometrical data of the structure, the properties of the soils, the reinforcing materials and they're of their interaction. The complexity of this phenomenon limits the use of analytical calculations.

A specific application of geosynthetics and which concerns the subject of this research thesis is embankment walls reinforced by geosynthetic elements to improve the resistance of the embankment supporting heavy loads, in particular road bridges. This series of complicated constructions includes the Reinforced Soil Retaining Wall with double facing (opposing walls) "Back-to-Back." According to the current report of the US Federal Highways and Highways Guidelines (FHWA 2009). The distance between the two opposite walls is a fundamental parameter used to identify the techniques of analysis, according to these instructions, and two extreme situations are identified:

- The two walls' reinforcements connect in the center or overlap;
- The walls are separate and unrelated to one another.

The objective of this research is to determine the effect of the overlapping-reinforcement (L_R) on the wall displacement, and the required tensile strength in reinforcement of back-to-back geosynthetic reinforced soil walls under self-weight.

ORGANIZATION OF THE THESIS

The thesis titled "***Behavior and design back-to-back mechanically stabilized earth walls***" consists of three Chapters. The thesis outline is presented below:

Chapter 1 presents a devoted to the generalities of soil reinforcement and reinforced earth structures (historical overview of soil improvement techniques, types of reinforced soil retaining structures, geosynthetic reinforcements, types of facing, implementation, etc.).

Chapter 2 deals with the relevant literature for the present research work, are briefly presented and discussed. Literature was reviewed on single reinforced retaining wall and back-to-back reinforced retaining walls. Then, the American FHWA 2009 guide for the design of reinforced soil structures is presented.

Chapter 3 describes the results of the reinforcement in back-to-back walls. A numerical model was developed to analyze the tensile forces mobilized in geogrid layers and the maximum displacements of BBMSE walls. The results were compared with the conventional Rankine.

FIRST PART

LITERATURE REVIEW

Chapter 1

Reinforced soil of mechanically stabilized earth walls

1.1 Introduction

Reinforced soil retaining walls are structures composed of structural (retaining walls) and geotechnical (soil reinforcement) elements. This construction technique has become popular since its invention by the French architect and engineer Henri Vidal in the early 1960s (Leshchinsky and Han, 2004). The construction method is based on the association of a compacted backfill and strip reinforcement elements connected to the wall facing. The reinforcements improve significantly the soil mass shear strength due to the soil-reinforcement interaction. The reinforcements generally used in these structures are made of steel (inextensible materials). However, in aggressive environments, these metal reinforcements are replaced by non-corrodible geosynthetic reinforcements, which have a higher extensibility than the metal ones. Reinforced soil walls constructed with geosynthetic reinforcements are considered in this dissertation. Traditionally, the analysis of reinforced soil retaining walls are based on deterministic approaches. However, all the input data are associated with some degree of uncertainty in geotechnical engineering problems.

1.2 Definition and historical background

A reinforced soil retaining wall is a low-cost soil-retaining construction made up of compacted backfill and reinforcement (metal or geosynthetic) elements attached to a wall facing (Figure 1.1). It's a composite structure made up of a frictional backfill made up of horizontally compressed layers between which reinforcing elements are positioned. Reinforced soil retaining walls, by behaving like coherent flexible blocks, can support larger loads and deformations than conventional reinforced concrete retaining structures. This significant technical advantage allows

their applications in areas where foundation soils are poor. In such cases, the foundation improvements to support conventional structures are not required which result in important cost savings. The reinforcements improve significantly the apparent soil shear strength due to the soil-reinforcement interaction by friction, and passive resistance depending on reinforcement geometry. The reinforcement's most common resisting mode is tension while some reinforcement types can also resist in bending and shear, providing additional stability to the reinforced soil structures (Alhajj Chehade, H. (2021)).

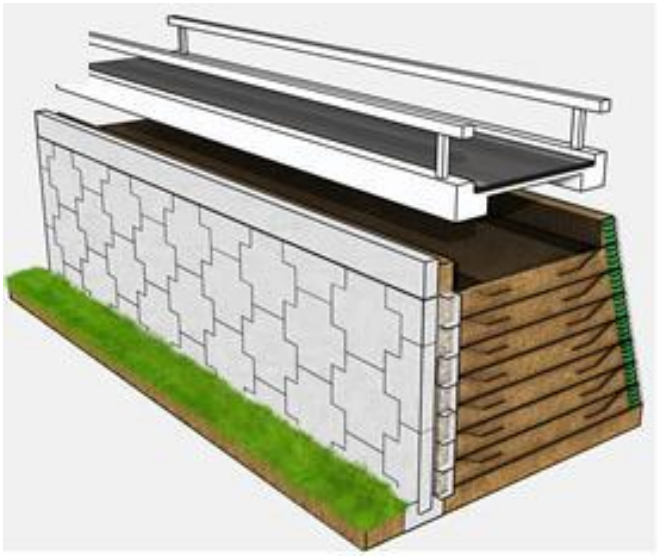

Figure 1.1 Reinforced Soil Retaining Wall.

The wall facing, relatively thin, prevents the erosion of the backfill soil. Sticks, earth dikes, tree branches, and wooden pegs, among other natural resources, have been utilized to enhance soil since ancient times. Henri Vidal, a French architect and engineer, devised current soil reinforcement technologies for retaining wall building in 1963, and they have since become common (Leshchinsky and Han, 2004). Henri Vidal's idea marks a watershed moment in the design of retaining structures, and more broadly, in soil strengthening, by fully engaging the soil in the structural stability. Sands and pine needles were used to test the concept of a reinforced earth retaining wall. His study led to the creation of the Reinforced Earth system, which employs steel strip reinforcement. In 1965-1966, the first reinforced earth retaining structure using metallic

materials was built in Pragnières (Pyrénées, France), with the construction of the first reinforced soil wall (Figure 1.2). The first one, which is still in use today in the United States, was built in California in 1972 utilizing this technique. Several more synthetic-reinforced systems have been created and deployed since the Reinforced Earth was first introduced. After its favorable effect was recognized in highway embankments constructed over poor subgrades, geotextiles began to be used in reinforced soil retaining walls. In 1971, the first geotextile-reinforced wall was built in France (FHWA, 2009). In addition, geogrids for soil reinforcement were first created in the 1980s (FHWA, 2009) (Alhajj Chehade, H. (2021)). The success of reinforced soil retaining walls can be attributed to their advantages over conventional retaining walls, such as their flexibility in the face of settlements and their ability to withstand seismic loading in seismically active areas (Ling et al., 2004-2005a-2005b; Koseki et al., 2006; El-Emam and Bathurst, 2007; Latha and Santhanakumar, 2015). These types of walls are now a mature technology that is widely used around the world. They are the first choice for the construction of retaining walls and highway infrastructure (Alhajj Chehade et al., 2019b) (Alhajj Chehade, H. (2021)).

Figure 1.2 First reinforced soil retaining wall constructed in 1965 by EDF (Chéret, 2015).

1.3 Types of reinforced embankment structures

Mechanically Stabilized Earth (MSE) walls, according to the American Association of State Highway and Transportation Officials (AASHTO), are earth retaining structures (Figure 1.3) that use either metallic (strip or grid type) or polymeric (sheet, strip, or grid type) tensile reinforcements in a soil mass and a vertical or near-vertical facing element (AASHTO, 1996). The dead weight of the composite soil mass behind the facing column restrains lateral forces as MSE walls behave as gravity walls. The comparatively thick facing's self-weight may also contribute to the overall capacity. Traditional gravity, cantilever, or counter fort concrete retaining walls may be prone to foundation settlement due to poor subsurface conditions, hence MSE walls are frequently employed (Leblanc, 2002). Figure 1.4 demonstrates different types of facing systems for geosynthetic reinforced soil (Bhuiyan, M. Z. I. (2012)).

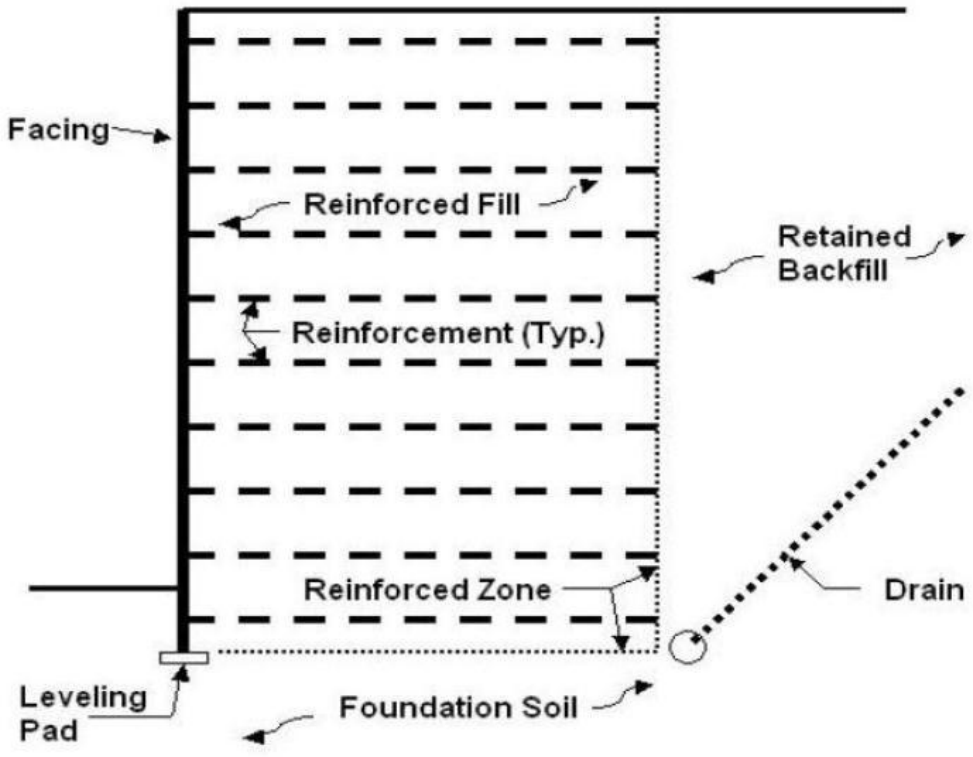

Figure 1.3 Cross section of a typical MSE structure (Berg et al., 2009).

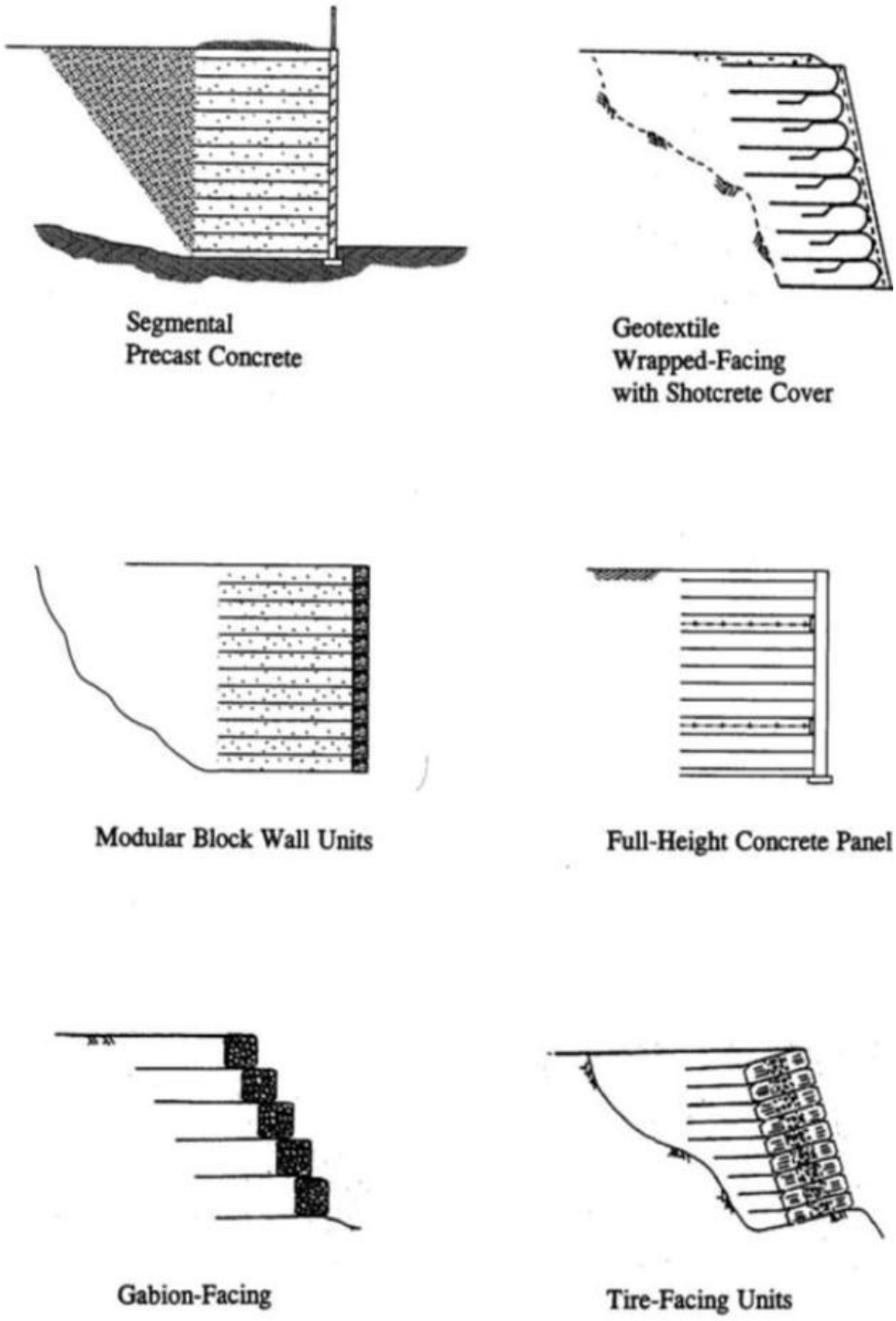

Figure 1.4 Facing types for geosynthetic reinforced soil wall (Berg et al., 2009).

1.4 Mechanically Stabilized Earth walls with metal reinforcement

1.4.1 Precast concrete facing panels

Concrete cruciform scales are the most widely `` panels (Figure 1.5). These are slabs weighing around 850 kg and measuring 1.5 meters in width and height. They are connected by a system of vertical dowels during installation to make assembly easier and assure the installation's continuity. The result is a vertical flexibility comparable to that of the metal pieces, which are thin curved plates originally created by Henri Vidal. Curved walls with regular scales are possible because to the ability to rotate around the studs. The exterior surface of the scales can be changed in shape, texture, and color to offer each wall a different architectural character.

Figure 1.5 Examples of cruciform facing panels.

1.4.2 Cast-in-place facing

Cast-in-place concrete is a construction technique that utilizes a temporary formwork to shape the concrete slurry until it hardens. It has many applications including housing construction, gutters, traditional open-trench pipeline construction, and the manufacture of concrete pipes used in the trenchless construction industry, as shown in Figure 1.6.

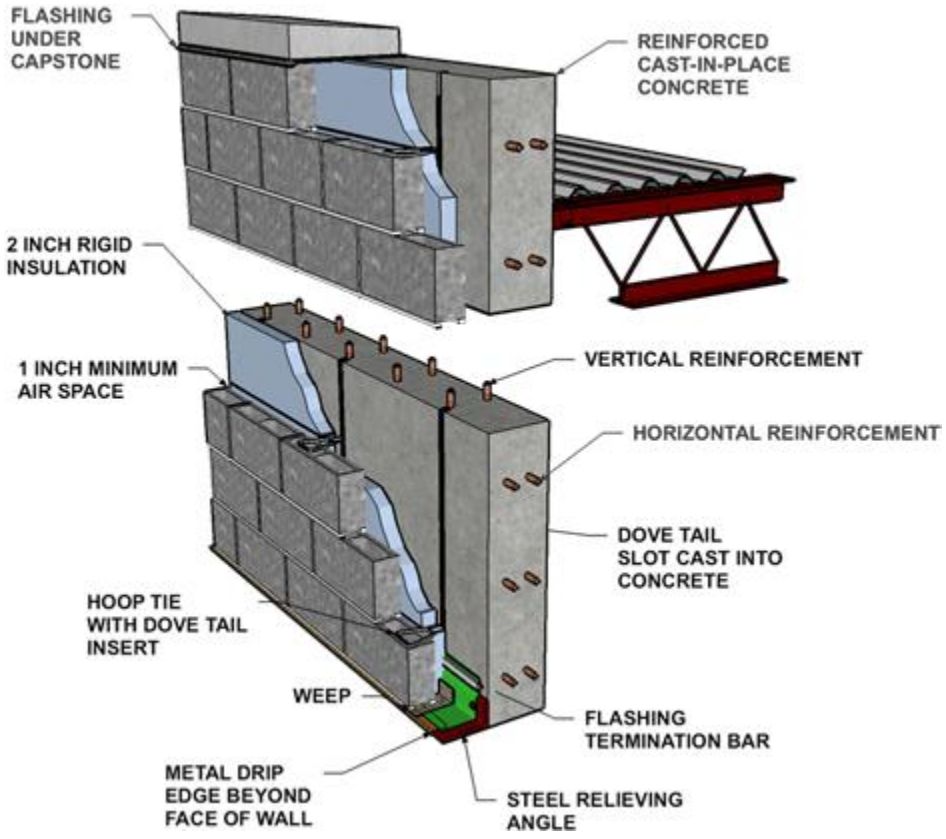

Figure 1.6 Display of cast-in-place concrete facing.

1.4.3 Modular block facings (Segmental retaining walls)

A segmental retaining wall (SRW) is erected from dry-stacked units (mortar-less) that are usually connected through concrete shear keys or mechanical connectors. Segmental retaining walls are divided into two groups according to soil reinforcement: conventional SRWs and reinforced soil SRWs. Conventional SRWs are structures that resist external destabilizing forces, solely through the self-weight and batter of the facing units. Reinforced soil SRWs are composite systems consisting of mortar-less facing units in combination with a reinforced soil mass stabilized by horizontal layers of geosynthetic or metallic reinforcements. Figure 1.7 shows schematic diagrams of SRW systems and their components. Reinforced soil SRWs are also referred as MSE walls. SRWs offer important advantages over other types of soil retaining wall systems due to their durability, outstanding aesthetics, ability to tolerate differential settlement, ability to incorporate curves or corners, ease of installation and economics.

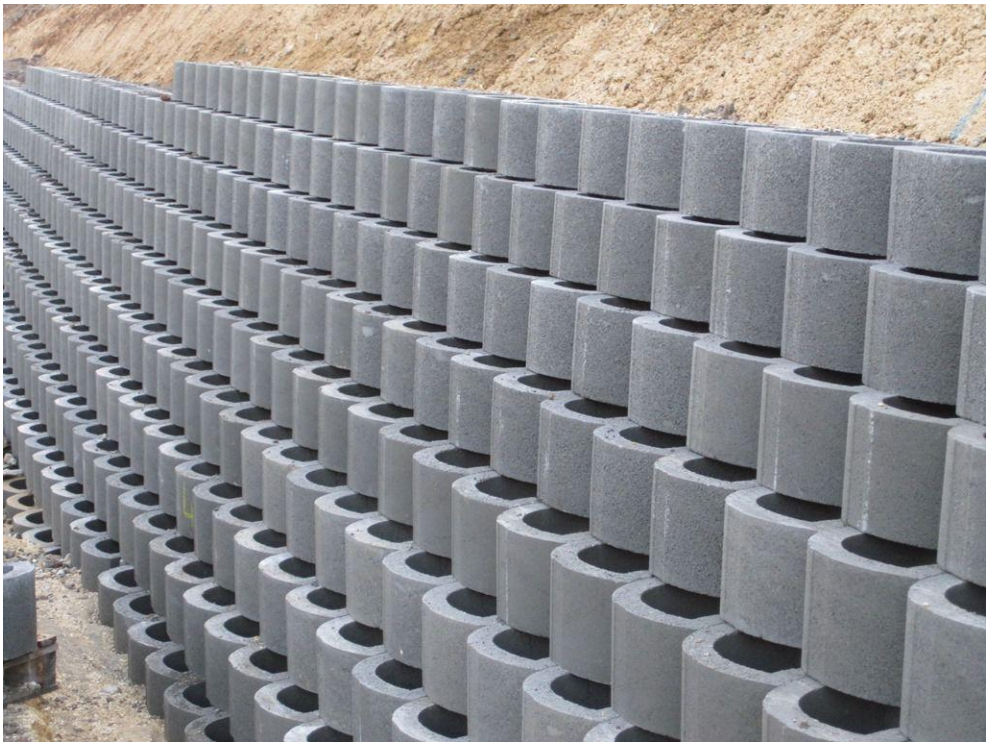

Figure 1.7 Segmental retaining wall systems.

1.5 Mechanically Stabilized Earth walls with geosynthetic reinforcement

1.5.1 Wrap-around facing

Using a pyramidal-woven, high-performance turf reinforcement mat (HPTRM) and fiber composite internal braces, new patented technology can be used to build geosynthetic wrap-face vegetated (GWFV) retaining walls and reinforced soil slopes, as shown in Figure 1.8. This wrap-face technology avoids the requirement for temporary external bracing (formwork) or metal wire-frame facing elements, which have historically served as a bulkhead to allow mechanical compaction of backfill soil directly behind the face. On-site soil can be used for infill in many circumstances, as long as it includes little organic debris and does not contain fine-grained elastic soil. Depending on the application and site conditions, vegetation can be seeded or planted during construction or afterward. The GWFV system is well-suited to stream-bank, wetland, littoral, and coastal applications, as well as landslide remediation and as wing walls for the building of a geosynthetic reinforced soil–integrated bridge system (GRS–IBS).

Figure 1.8 Wrap-Around Reinforced Retaining Wall for Collapsed Slope

1.5.2 Gabion facing

Gabion facing are built primarily for soil stabilization behind the wall, although they can also be used as a cover wall. The wall is constructed of gabion baskets placed in one or more rows, depending on the wall's height. Baskets are cage-shaped and have all four sides closed. They're comprised of galvanized hexagonal meshes and brocken rock put in baskets. Retaining structures are made by stacking gabion baskets in a specific order, and they are a good alternative to concrete buildings for soil stability (see Figure 1.9).

Gabion walls have an application mostly in road engineering, e.g. construction of roads, embankments, retaining walls, slope protection, water barriers etc., and can have different functions:

- Creation of a barrier that prevents soil erosion in coast and embankment stabilization.
- Prevention of sliding and washouts.
- Water speed reduction in prevention of soil erosion in water ways.
- Noise protection.
- Aesthetic fence structures for gardens.

Figure 1.9 Example of gabion walls.

1.5.3 Precast full-height concrete facing

Precast concrete is a type of construction product made by pouring concrete into a reusable mold or "form," curing it in a controlled environment, then transporting it to the job site and maneuvering it into position; examples include precast beams and tilt-up wall panels. Cast-in-place concrete, on the other hand, is poured into site-specific moulds and cured on location.

The cores of precast wall panels have recently been made of lightweight expanded polystyrene foam, which saves weight and improves thermal insulation. The finer aggregate used in the combination distinguishes precast stone from precast concrete, resulting in a product that resembles genuine stone (see Figure 1.10).

Figure 1.10 Modular precast concrete facing for soil-nailed retaining walls.

1.5.4 Cast-in-place full-height facing

The cast-in-place concrete facing is connected with the wrap-around reinforced structure behind by steel bars; the overall structure hence possesses advantages of both rigid and flexible structures. Cast-in-place concrete can be economically feasible. Much of the cost factor is related to the depth of a repair. Shotcrete is a good option when repair sections range in thickness from 15 to 30 cm. Either of these two options is usually cost-effective. Thicker sections of concrete require traditional concrete forming to maintain the cost-effectiveness (see Figure 1.11). The minimum width that normally dictates the need for a form is 30 cm. Conventional cast-in-

place concrete offers a number of advantages over other rehab materials. Some of these advantages include:

- It can be proportioned to stimulate existing concrete substrate.
- It can minimize strains resulting from material incompatibility.
- Admixtures can be used in freezing and thawing temperatures.
- Conventional concrete using proven methods that equipment and skilled workers are available for.

Figure 1.11 Example of Cast-in-place Concrete.

1.5.5 Segmental concrete walls (SRWs) (modular block facings)

Segmental retaining walls consist of modular concrete blocks that interlock with each other. They are used to hold back a sloping face of soil to provide a solid, vertical front. Without adequate retention, slopes can cave, slump or slide. With the unique construction of segmental retaining walls, higher and steeper walls can be constructed with the ability to retain the force of lateral earth pressure created by the backfill soil (Figure 1.12).

Segmental retaining walls can be installed in a wide variety of colors, sizes, and textures. They can incorporate straight or curved lines, steps, and corners. They are ideal for not only slope support, but also for widening areas that would otherwise be unusable due to the natural slope

of the land. Retaining walls are often used for grade changes, and for other functional reasons such as widening driveways, walkways, or creating more space in a patio outdoor area.

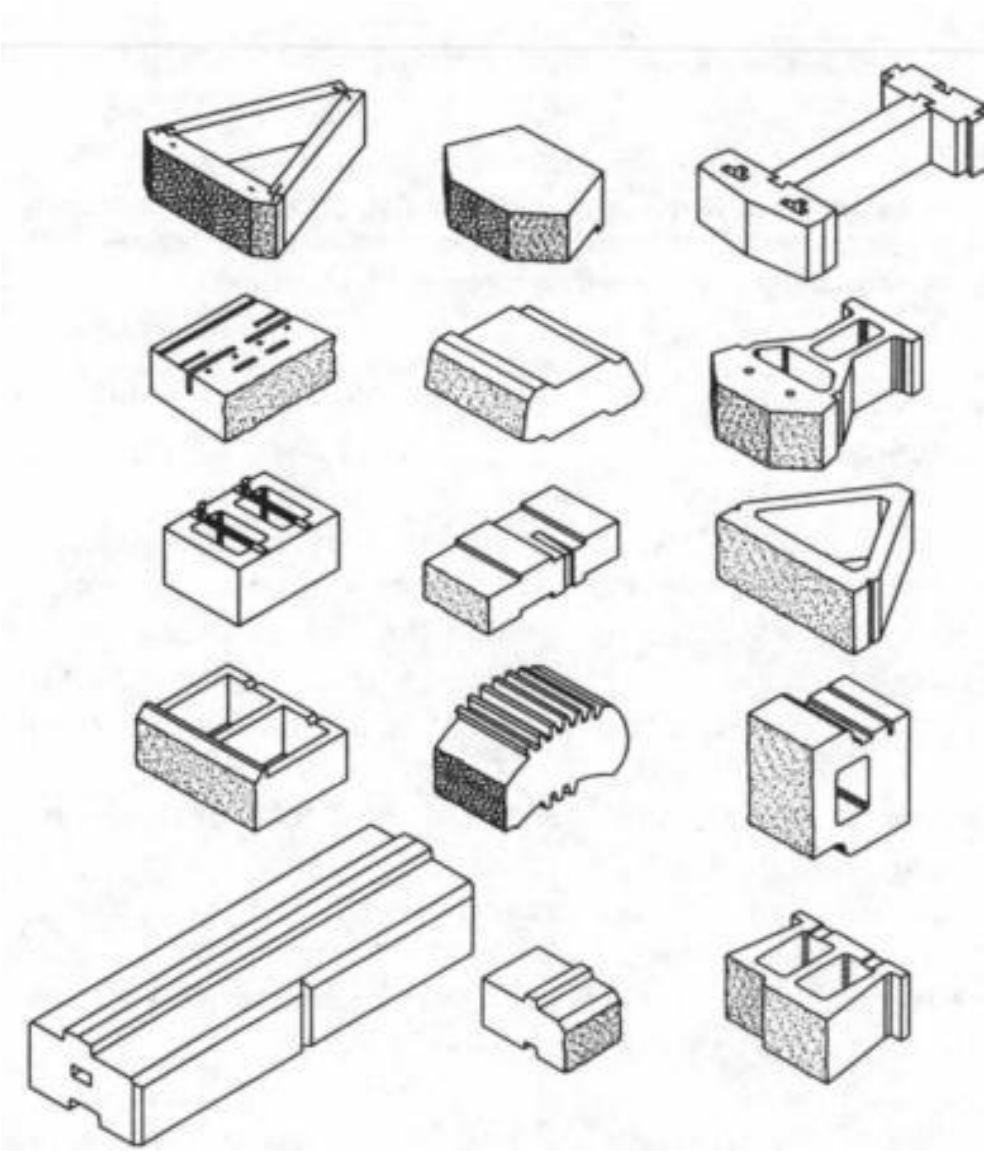

Figure 1.12 Examples of segmental retaining wall units.

1.6 Reinforcing elements

Reinforced soil structures (Figure 1.13) are made up of compacted layers of soil 50 to 150 cm thick with reinforcing elements of appropriate length interposed to improve overall resistance; the external face of the structure is protected by a facing made up of shotcrete and wire mesh, geogrid/geotextile sheets, modular facing blocks, cast-in-situ or prefabricated panels, or other similar materials (Figure 1.4). Biotechnical elements may be used into the facing for aesthetic considerations solely.

The reinforcing elements may consist of:

- Metallic strips (Reinforced Earth or Terre Armée);
- Polymeric strips;
- Geotextile
- sheets;
- Geogrids;
- Metallic grids.

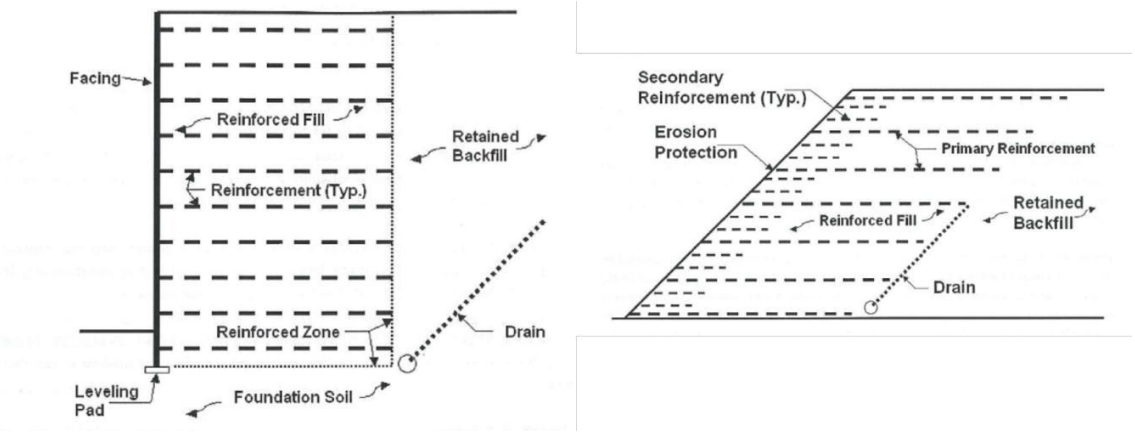

Figure 1.13 Generic cross section of reinforced soil walls and slopes (source Berg et al., 2009).

1.6.1 Metallic and Polymeric

The reinforcements are employed to strengthen the soil and provide the necessary tensile strength to keep it together. MSE walls use two types of reinforcing elements. Metallic and polymeric reinforcements are used. Galvanised iron ribbed strips (50mm-100mm) or ladder strip arrangements are examples of metallic reinforcements (in-extensible).

Polymeric reinforcement (Extensible reinforcement) could be geo-grids or geo-textiles, which are preferred in corrosive environments. For any vertical and horizontal obstructions, reinforcements are bend at an angle, not more than 15 degrees (refer Figure 1.14 and 1.15).

Figure 1.14 Metal reinforcing bars.

Figure 1.15 Type of reinforcement geogrids.

1.6.2 Geotextiles

Geotextiles are synthetic materials that are permeable and are used in conjunction with the soil mass. Polymers such as polypropylene and polyester are commonly used. Woven fabrics, nonwoven fabrics, and knitted fabrics are the three most common types (Figure 1.16).

Woven Geotextiles: The weaving process is used to create woven geotextiles. Its appearance can be separated into two distinct yarns: the warp, which runs parallel to the length, and the weft, which runs perpendicular to the length. Individual threads (monofilaments, fibrillated yarns, slit films) are intertwined to create a huge, homogeneous piece. This process gives the geotextiles a high load capacity, making them ideal for road construction.

Non-Woven Geotextiles: Short staple fiber or continuous filament yarn are used to make nonwoven geotextiles. These geotextiles are manufactured/bonded together utilizing thermal, chemical, or mechanical processes rather than weaving. Thermally bonded non-wovens have a wide range of aperture widths and a typical thickness of about 0.5-1 mm, whereas chemically bonded non-wovens are typically 3 mm thick. Mechanically bonded nonwovens, on the other hand, typically have a thickness of 2-5 mm and are also rather heavy due to the huge amount of polymer filament required to create a sufficient number of entangled filament cross wires for adequate bonding. Non-woven geotextiles are often unsuitable for tasks requiring stability or reinforcement.

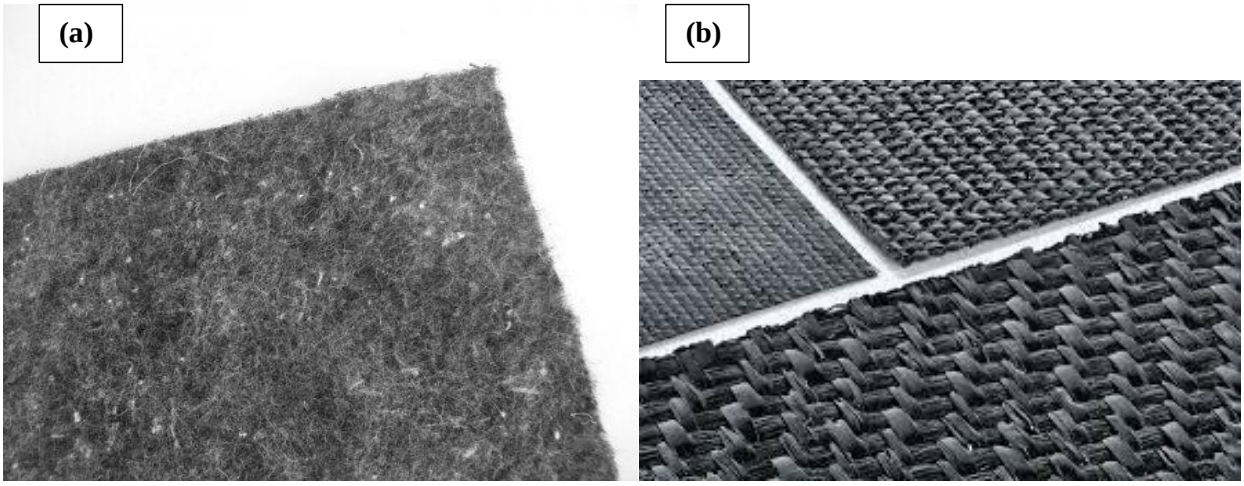

Figure 1.16 (a) Woven Geotextile and (b) Non-Woven Geotextile.

1.6.3 Jointing and filling materials

Rubber or wooden bearing pads are used between horizontal joints of facing elements so that there shall not be any concrete to concrete joints. The interior panel joints are sealed with geotextile filler cloth in the horizontal and vertical directions as shown in figure 1.17. This is done to ensure that no interior back fill materials sweep through the joints.

Figure 1.17 Example jointing materials for MSE walls (https://vincivilworld.com).

1.7 Advantages of Mechanically Stabilized Earth (MSE) wall

Advantages in terms of economy, ease of construction and rapid and speedy construction with minimum disturbances to traffic and other services makes MSE walls one of the most favourites and preferred retaining wall system. A variety of materials and customisation options in terms of design and construction made it one of the most popular earth retaining system. The fascia elements, the back-fill, and the reinforcing system combine to form a gravity retaining structure that relies on the self-weight of the reinforced soil mass. This self-weight resists the lateral pressure from the earth and the service loads, seismic loads, and hydro static pressure.

- They can be designed to take extremely heavy loads like bridge abutment footings, crane loads, service loads, etc
- MSE walls can resist seismic and dynamic forces and transfers the bearing pressure to a wide area.
- Faster construction than conventional retaining walls.
- Less site preparation is required and can be constructed in confined areas where other retaining walls are impossible to construct.
- There are no supports, finishes and curing time.
- The granular back filling enables free drainage of water through the exposed panel joints and reduces hydro static pressure.
- The fascia walls are lightweight and are precast and conveyed to the site and lifted using simple lifting equipment. These walls can be made to any height and can resist unequal settlements
- They can be customised to any geometry and the construction process is very simple. They do not need any heavy types of machinery and specialised workers.
- The fascia can be customised for designs and logos and gives superior and elegant finished and aligned walls.
- Any obstructions inside the back filled areas can be managed by adjusting the angle of the reinforcing elements.
- They possess a very good service life in extreme loading and complex applications.

1.8 Disadvantages of Mechanically Stabilized Earth (MSE) wall

The retaining walls (MSE) require granular material in huge quantities. Areas where there is a scarcity of granular material the construction cost increase and make the structure uneconomical.

- The corrosion or reinforcement and deterioration of geo-grids on exposed to sunlight has to be addressed. The reinforced component must be designed to withstand erosion and corrosion processes which can highly deteriorate the mechanical behavior of the composite structure.
- Proper drainage system should be provided.
- The wall must obtain a minimum width in order to acquire adequate stability

1.9 Conclusion

This chapter has demonstrated that there is a wide range of reinforced soil support options. It's ideal for the following scenarios:

- When compared to a normal embankment, the right-of-way is reduced.
- When the soil support has insufficient mechanical characteristics (risques of tassements généraux or differentiels, low portance that would require pieux for a concrete ouvrage, etc.), a remblai expansion with a mi-talus foundation is an alternative to a traditional wall.
- Possibility of using materials with a higher fines content (with particular precautions) in the event of continuous remblais, as opposed to armatures or bands.
- Integration on-site for slanted and vegetated lots.
- When compared to a traditional solution of reinforced concrete and a curved wall, the use of this approach resulted in significant cost savings.

The recent surge in the construction of reinforced concrete structures has prompted the updating of user guides and standards, which will be the subject of the next chapter.

Chapter 2

Analysis of geosynthetic-reinforced soil retaining walls

2.1 Introduction

This chapter provides a thorough and critical review of the performance of reinforced soil based on previously published studies. This Chapter presents key research studies available on the topic and is divided into two main parts: (a) review on the single-reinforced retaining wall, (b) review on back-to-back reinforced retaining walls.

2.2 Analysis of single-reinforced retaining walls

2.2.1 Experimental Studies

2.2.1.1 Shaking Table Tests

Richardson and Lee (1975) used shake table tests on a small-scale model of a 380 mm height reinforced soil wall with aluminum strips to conduct the first known study of the behavior of reinforced earth walls under dynamic loads. It was recommended that much more work be needed to understand aspects of the behavior of reinforced walls under seismic load conditions. Sakaguchi (1996) performed reduced scale shake table tests on 1.5 m high reinforced soil models with a wrapped face and lightweight modular block forms. The effects of geosynthetic length, soil density, and strength on the magnitude of horizontal wall displacements of geosynthetic reinforced retaining walls under seismic loading were investigated. It has been reported that the maximum displacement of the wall has decreased significantly by increasing the reinforcement layers. Koseki et al. (1998) carried out shake table tests on models of reinforced soil walls with rigid facing and conventional retaining walls of 0.5 m high. They observed that the critical acceleration related to lateral displacement was equal to 5% of the wall height, with an increase of about 20% when the length of the upper reinforcement layer was increased by a factor of four and the fourth layer by a factor of 2.25 (Figure 2.1 and 2.2). Matsuo et al. (1998) performed shake table tests on six scaled-down models of soil walls reinforced with geogrids to observe the behavior and reinforcement mechanism that happens in GRS. The model walls were 1m and 1.4m high with discrete and continuous panels as facing,

and different ratios of length reinforcement to wall height (i.e. ratio L/H from 0.4 & 0.7). Five model walls were subjected to sinusoidal motion and one model wall was subjected to the Kobe earthquake. The analysis noted that increasing the reinforcement length ratio L/H from 0.4 to 0.7 was a more efficient method of lessening wall deformation.

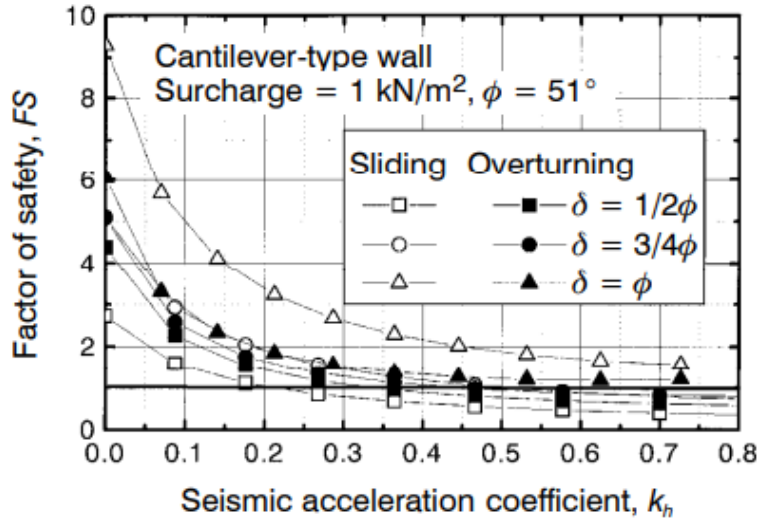

Figure 2.1 Predicted factors of safety for a model cantilever-type retaining wall during shaking table tests (Koseki et al.1998).

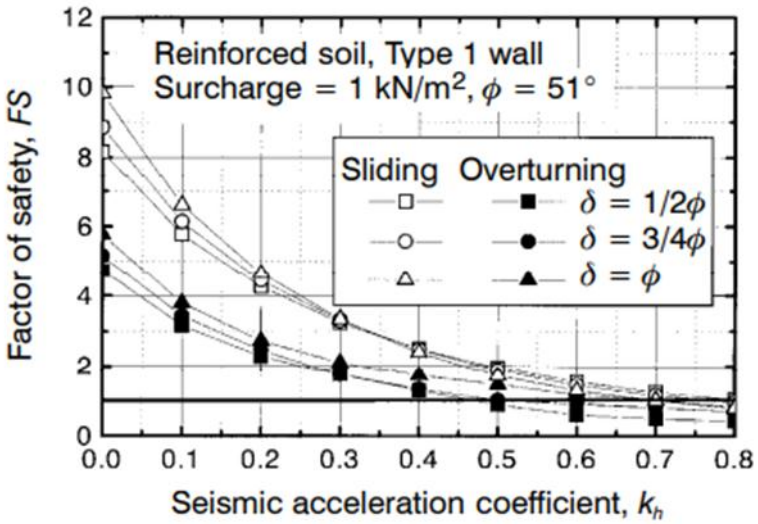

Figure 2.2 Predicted factors of safety for a model reinforced soil; Type 1 retaining wall during shaking table testes (Koseki et al.1998).

The effect of reducing the reinforcement L/H ratio leading to an increase in wall displacement has also been confirmed in other model studies (El-Emam and Bathurst, 2007). El-Emam and Bathurst (2007) It was found that reducing the L / H ratio by 40% for L / H = 1 to L / H = 0.6 increased the maximum lateral displacement by approximately 30% at 0.32 g base acceleration (refer Figure 2.3). This observation agrees well with Sakaguchi et al. (1992) who reported a 40% decrease in lateral displacement.

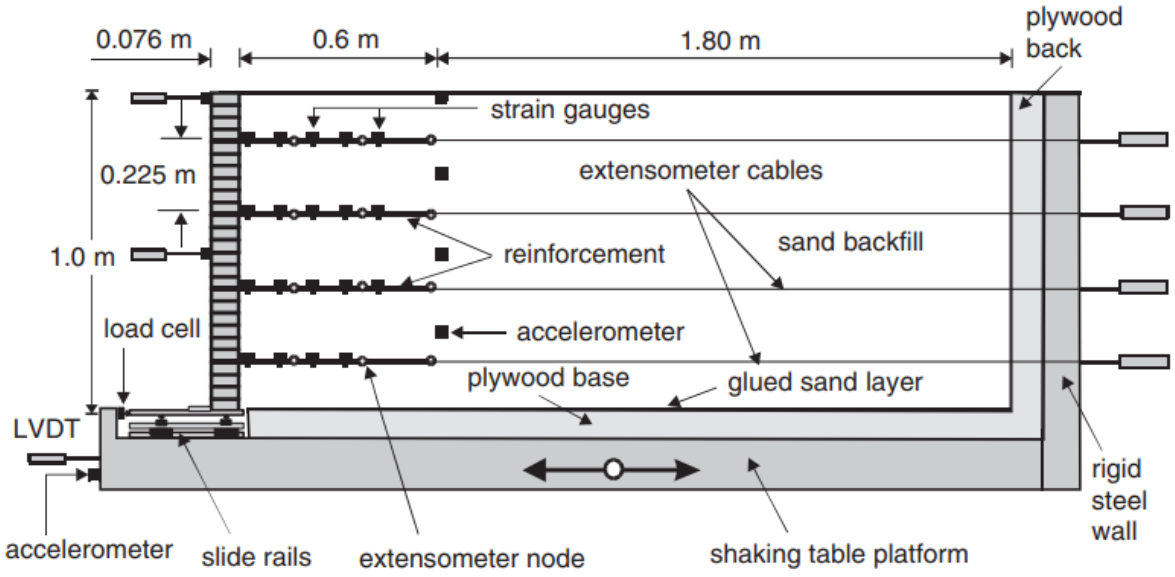

Figure 2.3 Cross-section arrangement and instrumentation layout of reduced-scale reinforced soil model walls (EL-Emam and Bathurst 2005).

Ling et al. (2005) conducted a full-scale shake table test on three walls of the GRS with modular block facing to study its seismic performance. The walls had a height of 2.8 m and had a 0.2 m thick foundation soil. The reinforcement spacing was 40 cm in two Walls 1 and 2 and 60 cm for Wall 3, every wall was subjected to a vertical acceleration, whereas Wall 3 was subjected to both horizontal and vertical of 0.4g followed by 0.8g, is shown in Figure 2.4. They concluded that using longer reinforcement at the top layer and smaller vertical reinforcement spacing under seismic load improved the seismic performance of GRS walls. Lateral displacement was also observed to be greatest at the top of the wall.

Krishna (2008) and Krishna and Latha (2007) conducted shake table tests on a 0.6 m-high model GRS walls reinforced with geotextile, to understand the influence of the relative density of the backfill soil on the seismic response of three different wall designs at acceleration levels

of 0.1 g and 0.2 g (refer Figure 2.5). In addition, retaining walls with facing panels experienced less acceleration compared to reinforced soil walls rigid facing.

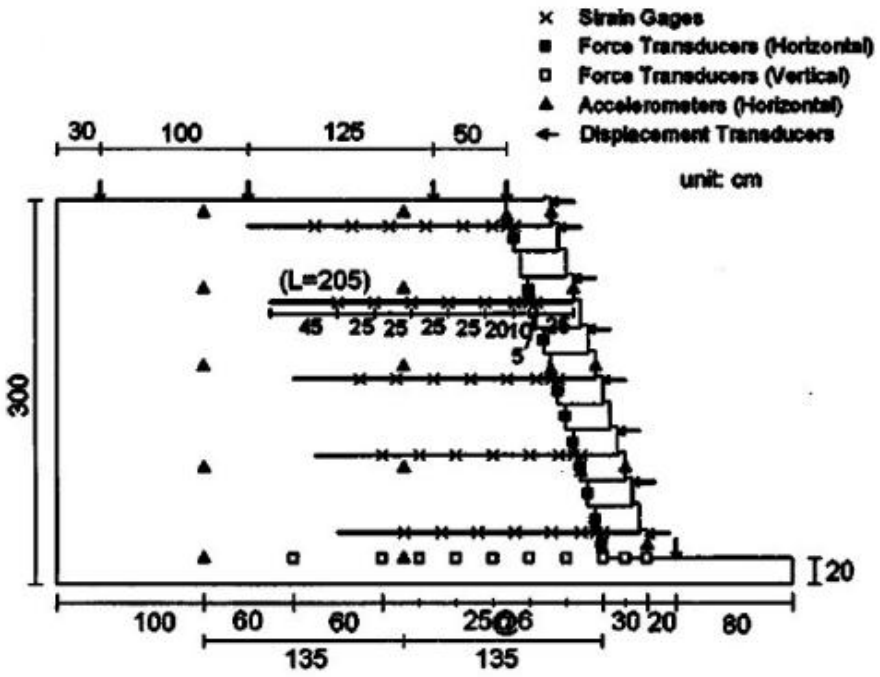

Figure 2.4 Cross-section instrumentation and layout of Wall 1 in full-scale shaking table tests (Ling et al. 2005a).

Comparable results have been reported by Nova-Roessig and Sitar (2006) in their studies on centrifuge models. However, retaining walls with facing panels experienced less acceleration compared to reinforced soil walls rigid facing. The influences of the relative density of the backfill on the seismic response of GRS walls were only pronounced at low relative densities and at higher base excitations.

In an experimental study by Krishna and Latha (2009) investigated the effects of reinforcement on the seismic performance of GRS walls with a full-height rigid facing. It was noted that the reduction in lateral displacements facing the wall compared to the measured displacements of unreinforced walls.

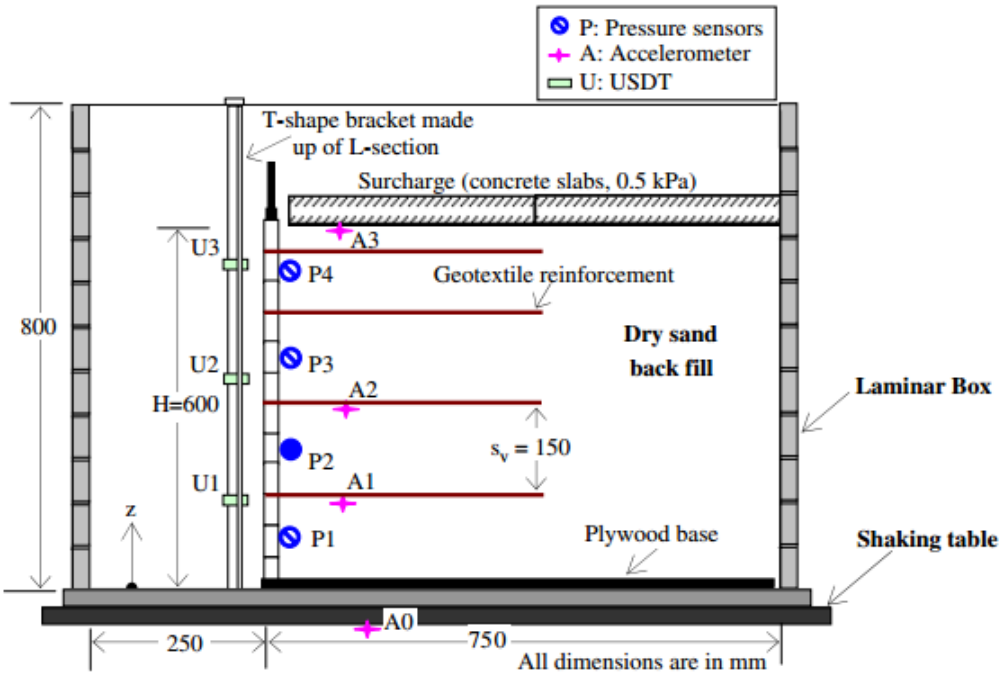

Figure 2.5 A schematic diagram of a typical rigid-faced wall configuration and instrumentation (Krishna and Latha 2007).

2.2.1.2 Dynamic Centrifuge Tests

Sakaguchi, M. et al. (1996) made centrifugal tests to investigate the effects of soil density, geosynthetic length and strength on the magnitude of horizontal wall displacements of geosynthetic reinforced retaining walls under earthquake loading. It was found that the maximum tensile force in the geotextile had a slight influence on the seismic responses of the walls, as the tensile forces developed during seismic effects were well below the particular tensile limits.

Takemura and Takahashi (2003) used centrifuge tests to investigate the influences of reinforcement length, vertical reinforcement spacing, and backfill dry density on the dynamic response of GRS walls. The prototype wall was 7.5 m high and was subjected to sinusoidal excitation. The dry low-density backfill wall specimen underwent greater horizontal translation and greater tensile strains in the reinforcement. Studies of centrifuge models by Siddharthan et al. (2004) on soil retaining walls reinforced with bar-mat subjected to seismic ground motions. The results of the tests showed that the maximum lateral displacement of the facing occurred at mid-height of the reinforced walls. However, walls with longer reinforcements underwent less deformation. Study different performance levels of retaining walls of reinforced geosynthetic soil with modular block facing, under different earthquake by Liu et al. (2010) conducted

dynamic centrifuge tests on three GRS walls. The results highlighted the importance of the overall acceleration and duration of the earthquake. The results highlighted the importance of the overall acceleration and duration of the earthquake. Under simple excitation, the acceleration within GRS walls amplified greatly, indicating that designing tall GRS walls against a modest seismic load may require considering a change in acceleration with height (refer Figure 2.6 and 2.7). Liu et al. (2010) proposed that the design of GRS high walls may need to account for the change in acceleration with height.

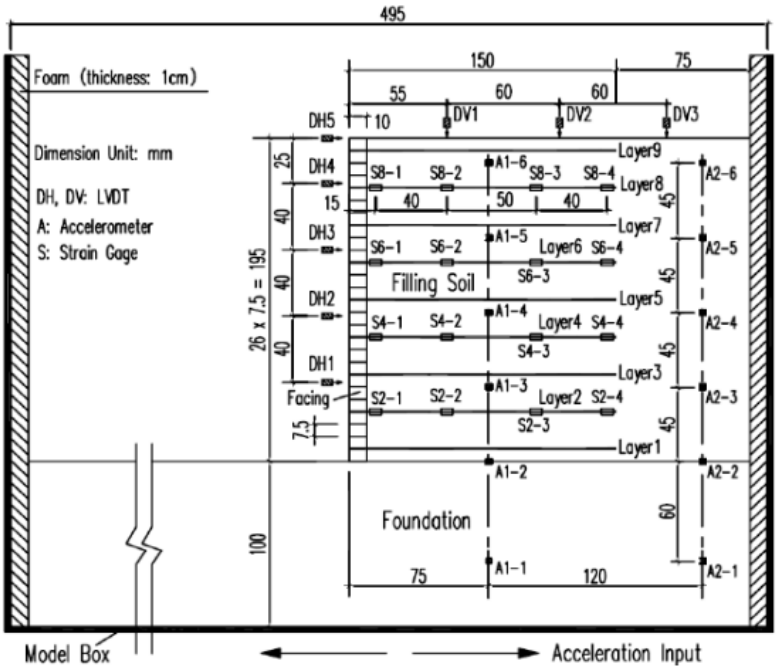

Figure 2.6 Setup of centrifuge model walls (Liu et al. 2010).

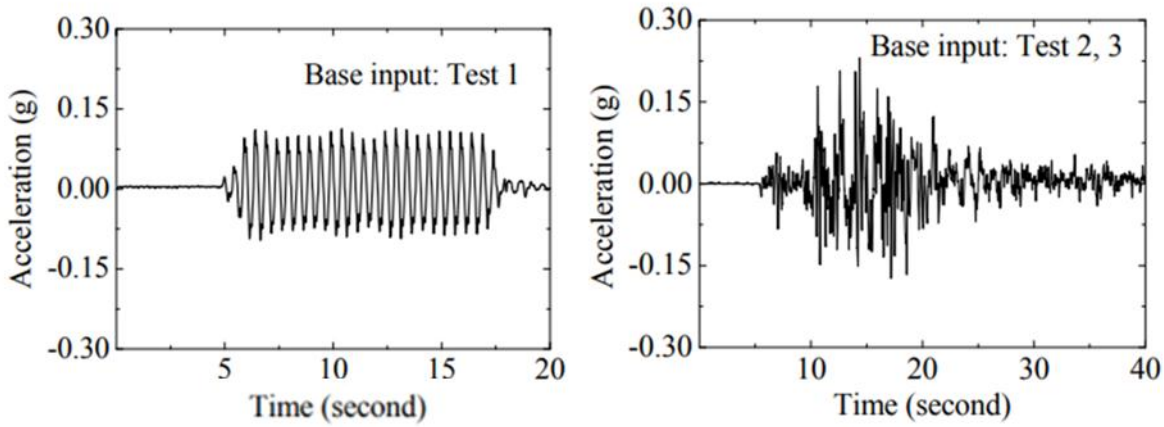

Figure 2.7 Input accelerations: (a) Test 1; (b) Tests 2 and 3 (Liu et al. 2010).

2.2.2 Numerical Studies

Segrestio and Bastick (1988) validated a dynamic finite element model generated using the program SUPERFLUSH using measured results from a shaking table test on a steel stripreinforced soil wall (Chida et al. 1985). Yogendrakumar et al. (1991) used the program TARA-3 to study the seismic response of 6 m-high retaining walls reinforced with steel strips. Yogendrakumar and Bathurst (1992) and Bachus et al. (1993) conducted dynamic finite element modeling of reinforced soil walls subjected to blast loading using the programs RESBLAST and DYNA3D, respectively. Yogendrakumar et al. (1992) studied the dynamic response of reinforced soil wall under blast loading using both equivalent linear approach and nonlinear incremental approach, and found that the nonlinear incremental approach gave better predictions when compared to measured results from a field test.

Cai and Bathurst (1995) investigated the dynamic response of a geosynthetic reinforced soil retaining wall with modular blocks using the finite element method. Reinforcement was modeled using a similar hysteretic model that took into account the measured response of cyclic load extension tests on unconfined geogrid specimens. An ElCentro earthquake recording scale (PGA = 0.25 g) was applied to the base of the GRS wall model. They achieved that an exact estimation of interface shear properties is especially important for the seismic design of retaining walls in segmental geosynthetic reinforced soil. Cai and Bathurst also noted that the dynamic tensile forces in the fixed reinforcement layers during simulated seismic results and the maximum tensile forces increased with the amplitude of the maximum acceleration of the base. The influence of boundary conditions and base acceleration records on the seismic response of a GRS wall using FLAC has been studied by Bathurst and Hatami (1998). They showed that the wall incremental loads increased with increasing reinforcement stiffness over a wide range of values that included relatively flexible geosynthetic reinforcement materials as well as metallic reinforcement.

Hatami and Bathurst (2000b) simulated the dynamic response of GRS walls with modular block facing subjected to different ground motions. Deformations and reinforcement forces for GRS walls subjected to a single frequency harmonic motion were larger than the responses of walls subjected to actual earthquake ground motions with comparable predominant frequencies. They also found that low-frequency ground motions with high intensity could result in significant structural responses of short-period GRS walls (Figure 2.8).

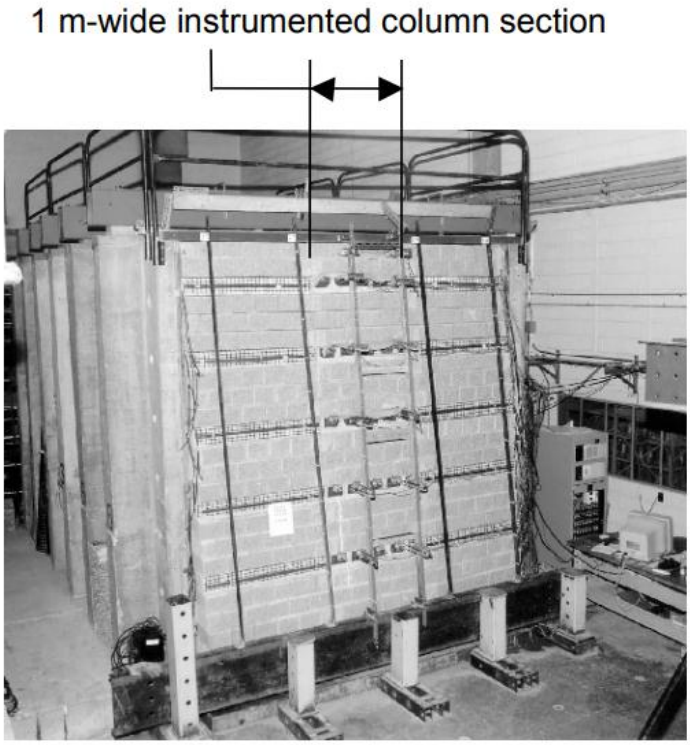

Figure 2.8 Example full-scale reinforced soil retaining wall (Hatami and Bathurst 2000).

Hatami and Bathurst (2000a) investigated the effect of different fundamental frequencies of a GRS structure of reinforced-soil retaining wall models. The design parameters in the study included the wall height, backfill width, reinforcement length, reinforcement stiffness, backfill friction angle, and toe restraint condition. Their numerical analyzes showed that fundamental frequency was not significantly influenced by reinforcement stiffness reinforcement length, conditions of restraint of the toes. The resistance of the granular backfill, characterized by its friction angle, also did not show any observable effect on the fundamental frequency of reinforced-soil retaining wall models.

Helwany et al. (2001) verified a finite element model generated using the program DYNA3D using measured results from a small-scale shaking table test on a 0.9 m high GRS segmental wall (Figure 2.9). Nonlinear hysteretic behavior of the backfill soil under cyclic loading was simulated using the Ramberg-Osgood model with parameters determined from laboratory tests. The geotextile was modeled as a linearly elastic material. Helwany and McCallen (2001) investigated the influence of facing block connection on the static and dynamic behavior of GRS walls with the validated model. At the end of construction, the wall using facing blocks with pin connections had smaller lateral facing displacement than the wall without pin connections, while the wall using facing blocks with pin connections experienced larger

seismic-induced displacements. Helwany and McCallen (2001) suggested that smaller seismic-induced lateral displacements in the wall without pin connections were due to smaller lateral earth pressures behind the facing, as the blocks without pin connections permit more relative sliding between blocks.

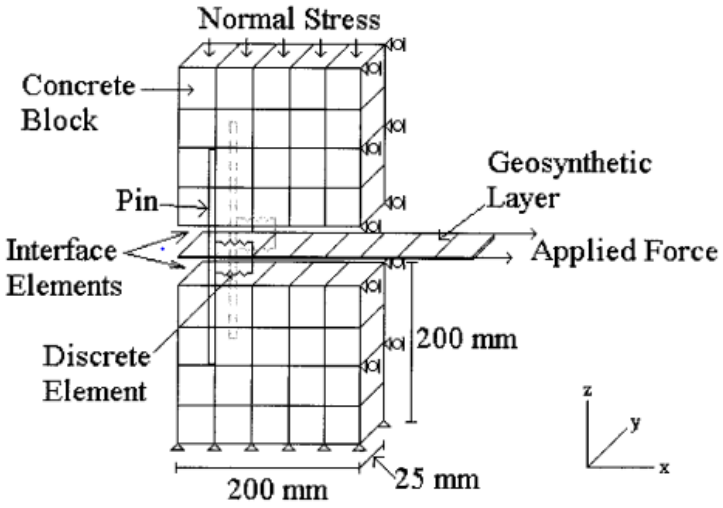

Figure 2.9 Finite-element discretization of large-scale connection test Helwany and (McCallen 2001).

Ling et al. (2004) validated a finite element model for both static and dynamic analyses using a modified version of Diana-Swandyne II. A generalized plasticity model which accounts for stress-dependent stiffness, strength and dilatancy, as well as cyclic hardening behavior, was used to characterize the backfill soil. A bounding surface model was used to simulate cyclic behavior of uniaxial geogrid. The interactions between different components were included using interface elements. The dynamic finite element model was validated using measured results from dynamic centrifuge tests. In these tests, the GRS walls were subjected to 20 cycles of sinusoidal excitation with a frequency of 2 Hz and acceleration amplitude of 0.2 g. Predicted accelerations, wall facing displacements, crest settlement and maximum tensile forces in the geogrid were compared with measured results, and showed good agreement.

Ling et al. (2005b) conducted a series of parametric studies using the validated finite element model to investigate effects of soil and reinforcement properties, reinforcement length and spacing, and block interaction properties on the performance of GRS walls at the end of construction and under earthquake loading. Lateral facing displacements and crest settlement were mainly influenced by soil cyclic behavior, reinforcement layout, and earthquake motions.

The effects of reinforcement vertical spacing on wall deformation, reinforcement forces, and lateral earth pressure were more significant than reinforcement length (Figure 2.10).

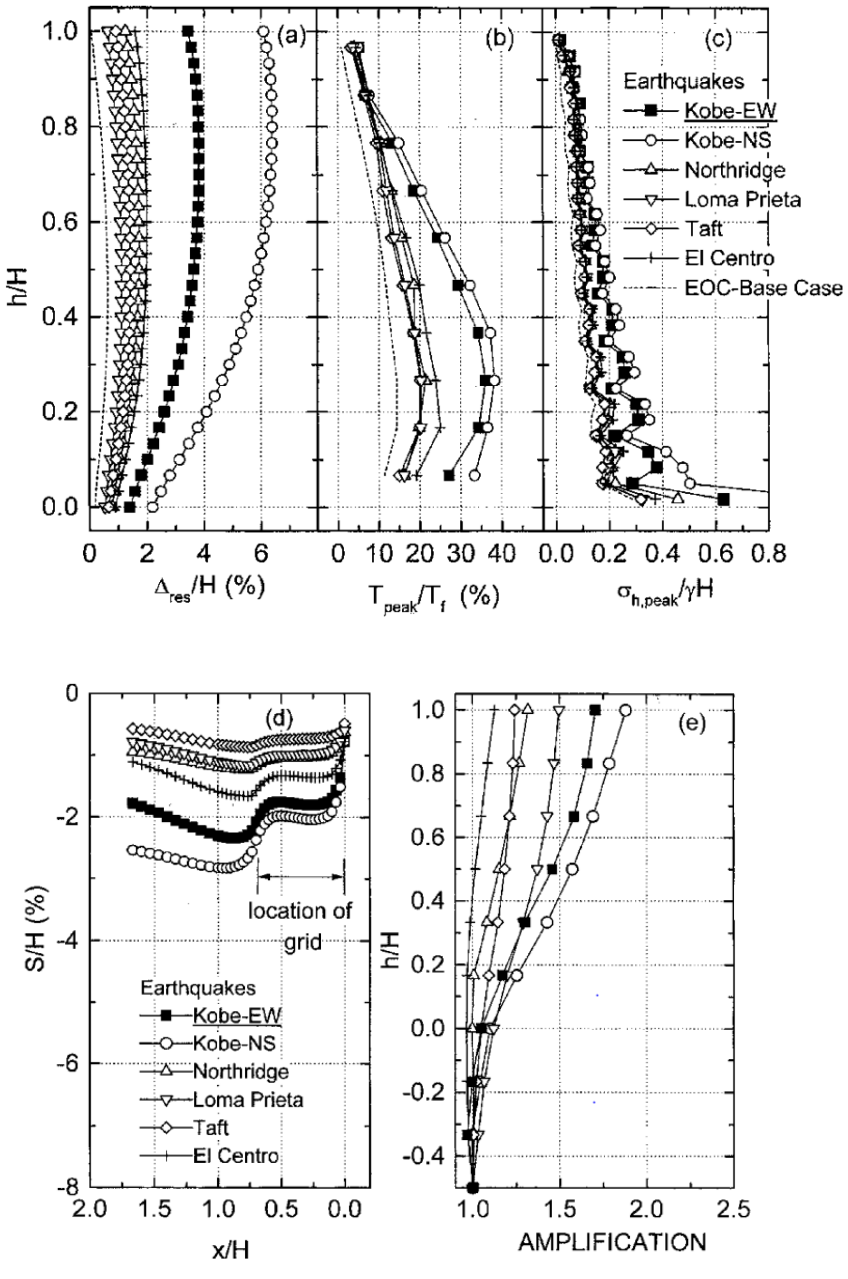

Figure 2.10 Effects of earthquake motions on seismic wall performance (a) facing lateral displacement ; (b) maximum reinforcement force (c) lateral earth pressure behind facing ; (d) crest surface settlement and (e) acceleration amplification.

Validated numerical models can be used to better understand the dynamic behavior of GRS walls. However, previous model validations have been based on either reduced-scale shaking table tests or dynamic centrifuge tests, both of which have disadvantages such as model size effects, stress level effects, and boundary condition effects. The full-scale shaking table tests on GRS walls with modular block facing (2.8 m high) conducted by Ling et al. (2005a) have provided data that can be used to calibrate dynamic numerical models. Ling et al. (2010) validated a dynamic finite element model using experimental results and improved soil and geosynthetic models based on their previous constitutive models (Ling 2003; Ling et al. 2005b). The unified general plasticity model for soil was improved by considering the effect of soil density, and the S-shaped load-strain relationship was accounted for in simulating the cyclic behavior of geogrid.

El-Emam et al. (2004) and Fakharian and Attar (2007) validated their FLAC models using measured results from reduced-scale shaking table tests on GRS walls conducted at RMC (El-Emam and Bathurst 2004; 2005). However, these validations are restricted to GRS walls with a rigid full-height facing panel.

Lee et al. (2010) also simulated full-scale shaking table tests using the finite element program LS-DYNA. The backfill soil was characterized using a geological cap model and the geogrid reinforcement was characterized using a plastic-kinematic model with a bilinear stress-strain curve. Lee and Chang (2012) conducted a series of parametric studies with their validated program to evaluate the effects of different design parameters, including wall height, wall batter angle, soil friction angle, reinforcement spacing, and reinforcement stiffness, on the seismic performance of GRS walls. The results showed that GRS walls become less stable with a decreasing batter angle (e.g., more near vertical) for the wall facing and a small vertical reinforcement spacing of 0.2 m is effective in decreasing wall deformations and reinforcement forces (Figure 2.11).

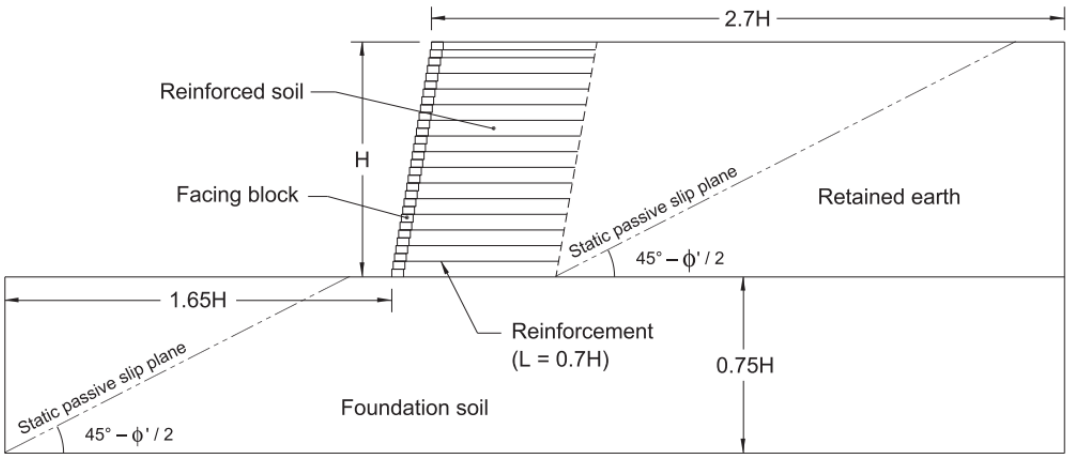

Figure 2.11 Numerical model dimensions adopted in the parametric study (Lee et al. 2010).

2.3 Design and Analysis of Geosynthetic-Reinforced Soil Retaining Walls

This section describes the current design and analysis of geosyntheticreinforced soil (GRS) retaining walls subjected to earthquake loads. In North America, a widely accepted design guidelines, which includes the seismic design of GRS retaining walls, is the Federal Highway Administration (FHWA) manual put forth by Elias et al. (2001). Another seismic design method for GRS walls follows the National Concrete Masonry Association (NCMA) manual (Bathurst 1998). Design of reinforced soil slope can be found in the US Army Corps of Engineers Waterways Experiment Station publication (Leshchinsky 1997). Other design methodologies from abroad have been surnrnarized by Zomberg and Leshchinsky (2003) and Koseki et al. (2006). Design criteria and analysis methods from the FHWA and NCMA manuals are surnrnarized as follows. The assumptions involved in the design are also presented.

2.3.1 Federal Highway Administration (FHWA) Methodology

Limit equilibrium (LE) method is adopted in the FHWA methodology, where one can only estimate the margins of safety against collapse and cannot estimate the deformation of the structure given the external loads. In the seismic design of GRS walls, the FHWA methodology requires both the external stability and the internal stability be evaluated in addition to the static design considerations. The design peak horizontal acceleration at a site can be obtained from Division I-A (AASHTO 2002) and Section 3.10 (AASHTO 2007) of the AASHTO Specifications. As specified by the FHWA methodology, the seismic design is needed whenever the peak acceleration coefficient (A) at the site being considered is greater than 0.05.

The coefficient is expressed as a fraction of gravitational constant, g, and is dimensionless. The maximum limiting value of A in which the FHWA seismic design requirements are applicable is 0.29, and the FHWA methodology recommends that the seismic design of a GRS wall should be reviewed by a specialist when A at the project site exceeds 0.29 (Lee, Z. Z. (2011)).

2.3.1.1 FHWA External Stability Evaluation

In the external stability evaluation for GRS walls, three potential modes of failure considered are: (1) base sliding, (2) eccentricity, (3) bearing capacity. Taking into account the flexibility/ductility exhibited by the GRS walls, the recommended minimum seismic factors of safety with respect to the failure modes are assumed as 75 percent of the static factors of safety, and the eccentricity should be within L/3 (L= length of the reinforcement) for both soil and rock foundations. Two forces in addition to the static forces in the external stability evaluation are the horizontal inertia force (PIR) and the seismic horizontal thrust increment (DPAE). DPAE is exerted on the reinforced soil by the retained soil. Both DPAE and PIR are shown in Figures 2.12 and 2.13 for level and sloping backfill conditions, respectively (Lee, Z. Z. (2011)). The seismic external stability is evaluated in the following steps:

- Select the acceleration coefficient A from Section 3 of AASHTO Division 1-A.
- Calculate the maximum acceleration (Am) developed within the GRS wall system.

Am = (1.45 - A)*A (2.10)

- Calculate the horizontal inertia force PIR and the seismic horizontal thrust increment DPAE. The height H2 should be used in finding PIR and DAE for sloping backfill condition (see Figure 2.13).

$$H_2 = H + \frac{\tan\beta.0.5H}{(1-0.5\tan\beta)} = \frac{H}{1-0.5\tan\beta} \quad (2.1)$$

The horizontal inertia force PIR is calculated as follows :

$$P_{IR} = P_{ir} + P_{is} \quad (2.2)$$

$$P_{ir} = 0.5A_m\gamma_f H_2 H \quad (2.3)$$

$$P_{is} = 0.125A_m\gamma_f (H_2)^2 \tan\beta \quad (2.4)$$

Note that Pir is the inertial force caused by acceleration of the reinforced backfill, and Pis is the inertial force cased by acceleration of the sloping soil surcharge above the reinforced backfill. The seismic horizontal thrust increment DP_{AE} is calculated using the pseudo-static Mononobe-Okabe method with the horizontal acceleration coefficient k_h equal to Am and vertical acceleration coefficient k_v equal to zero (Lee, Z. Z. (2011)).

The total seismic earth pressure coefficient K_{AE} is calculated following the general Mononobe-Okabe expression:

$$K_{AE} = \frac{\cos^2(\phi + \omega - \xi) / \left[\cos\zeta \cos^2\omega \cos(\beta - \omega + \xi)\right]}{\left[1 + \sqrt{\frac{\sin(\phi + \beta)\sin(\phi - \beta - \xi)}{\cos(\beta - \omega + \xi)\cos(\omega + \beta)}}\right]} \tag{2.5}$$

where, ϕ = peak soil friction angle, β = backfill surface slope angle from the horizontal, ξ = seismic inertial angle given by $\xi = tan^{-1}(k_h/1 \pm k_v)$, and k_h and k_v are the peak horizontal and vertical seismic coefficients, respectively.

The seismic earth pressure coefficient associated with the seismic thrust increment (DP_{AE}) is DK_{AE}, and $DK_{AE} = K_{AE} - K_A$. Note that the mobilized interface friction angle δ is assumed to be equal to β in the FHWA method. Note also that the wall batter angle 0) in the FHWA method is with the facing blocks inclined into the backfill, which is the opposite of the Coulomb method (Lee, Z. Z. (2011))..

Check factors of safety against failures of base sliding, eccentricity and bearing capacity with P_{IR} and 50% of DP_{AE}. The reduction of 50% on DP_{AE} was reasoned with possible phase lag between the inertial force and the seismic thrust from the retained backfill (Lee, Z. Z. (2011))..

For level backfill condition ($\beta = 0^0$), $H_2 = H$, $P_{is}=0$, and $P_{IR} = P_{ir}$

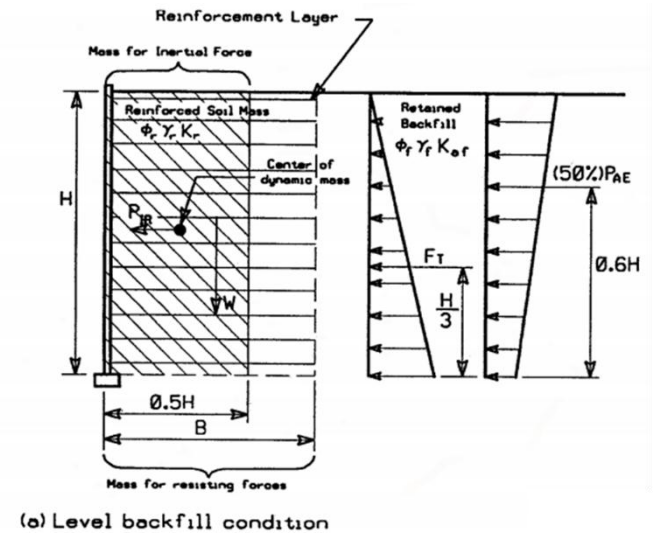

Figure 2.12 Seismic external stability of a GRS wall with level backfill in FHWA method.

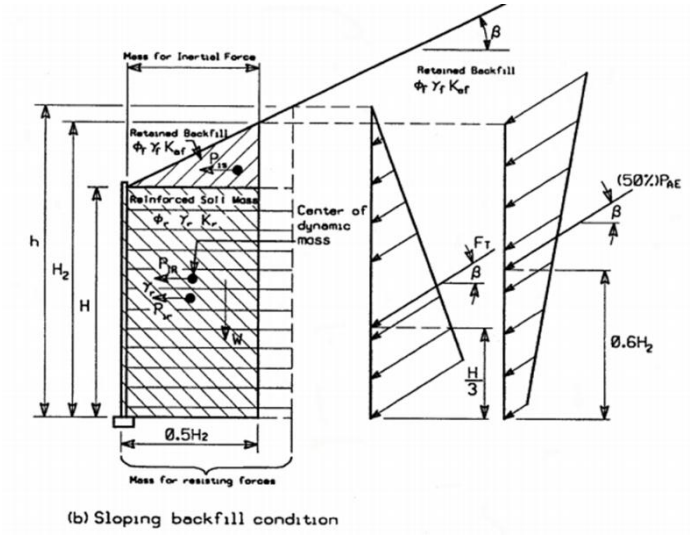

Figure 2.13 Seismic external stability of a GRS wall with sloping backfill in FHWA method.

As indicated by the FHWA manual, the use of full value of Am for kh in the pseudo-static Mononobe-Okabe method to find PAE can result in an excessively conservative design (Lee, Z. Z. (2011)). To achieve a more economical GRS wall, a reduced kh can be used if the following conditions are met:

- The wall is unrestrained regarding its ability to slide, other than soil friction along its base and minimal soil passive resistance.
- If the wall functions as an abutment, the top of the wall must also be unrestrained, e.g., the superstructure is supported by sliding bearings. With the conditions listed above and

provided that the GRS wall can tolerate displacements up to 250·A (mm), kh may be reduced to 0.5·A (i.e., kh = OSA).

FHWA methodology also provides an alternative method for estimating the horizontal acceleration coefficient kh in finding L1PAE . kh can be computed as:

$$K_h = 1.66Am\left(\frac{Am}{d}\right)^{0.25} \tag{2.6}$$

where d is the anticipated lateral wall displacement in mm. Noted that this equation should not be used for displacement of less than 25 mm or greater than 200 mm.

FHWA manual suggests that typical anticipated lateral wall displacement in seismically active area ranges from 50 mm to 100 mm.

It is to be noted that although a trapezoidal dynamic pressure distribution was proposed by the FHWA methodology (see Figures 2.12 and 2.13), and the actual dynamic pressure distribution was not specified. The equation for determining the seismic horizontal thrust increment DP_{AE} has otherwise suggested a triangular dynamic pressure (hydrostatic) distribution. For the seismic thrust to be located at 0.6H and with a trapezoidal pressure distribution, the ratio of long length (at the top) to the short length (at the bottom) of the trapezoid needs to be 4 (Lee, Z. Z. (2011)).

2.3.1.2 FHWA Internal Stability Evaluation

The internal failure of a GRS wall can occur in three ways: (1) pullout of reinforcement, (2) reinforcement rupture, and (3) connection pullout failure. To evaluate the internal stability of a GRS wall, one needs to determine the maximum developed tensile force in each reinforcement layer, the critical slip surface, and the resistance provided by the reinforcements in the resistant zone. It is assumed that the critical slip surface coincides with the locus of the maximum tensile force in each reinforcement layer Tmax, and the critical slip surface is further assumed to be linear in the case of extensible reinforcements which passes through the toe of the wall (see Figure 2.14). Also assumed is that the location and the slope of the linear critical slip surface is not affected by the seismic loads (i.e., the seismic critical slip surface is the same as the one for the static condition) (Lee, Z. Z. (2011)). The critical static slip surface, following the Coulomb's active condition, is inclined at an angle α_A from the horizontal as:

$$\alpha_A = \phi + \tan^{-1}\left[\frac{-\tan\phi - \beta + C_1}{C_2}\right] \tag{2.7}$$

As has mentioned earlier, in the FHWA methodology, the mobilized interface friction angle δ is assumed to be equal to the backfill slope angle p (i.e., $\delta = \beta$).

The static maximum tensile force in each reinforcement Trnax is a function of horizontal stress at each reinforcement level along the critical slip surface (σ_H) and reinforcement spacing (Sv), and T_{max} is computed as:

$$T_{\max} = \sigma_H . S_V \tag{2.8}$$

Furthermore, the horizontal stress σ_H is a function of the overburden stress, uniform surcharge loads, and concentrated surcharge loads. Alternatively, the tributary area from horizontal stress distribution can be used to calculate Tmax for each of the reinforcements. Note that the reinforcement spacing should not exceed 800 mm as required by the FHWA methodology.

In a seismic event, seismic loads would produce an inertial force PI acting horizontally in addition to the static forces (see Figure 2.14). The inertial force PI is calculated as:

$$P_I = A_m . W_A \tag{2.9}$$

where W_A is the weight of the active zone (shaded area in Figure 2.14), and Am is the maximum acceleration. Each reinforcement layer would receive additional seismic tensile force induced by the inertial force PI. The additional seismic tensile force T_{md} in each reinforcement layer is determined by proportionally distributing the PI based on the embedment length of reinforcements in the resistant zone and is computed as follows:

$$T_{md} = P_I \frac{L_{ei}}{\sum_{i=1}^{n} L_{ei}} \tag{2.10}$$

where n is number of reinforcement layers in the GRS wall. Knowing T_{max} and T_{md}, the total tensile force in each reinforcement layer T_{total} is calculated as:

$$T_{ult} = S_{rs} + S_{rt} \tag{2.11}$$

T_{total} is then used to evaluate the reinforcement pullout failure. Note that the factor of safety against reinforcement pullout failure FS_{po} under static condition should be greater than or equal to 1.5, and in seismic design, the factor of safety is said to be 75% of the static value. The total

tensile force in each reinforcement layer Ttotal should not exceed the pullout resistance Pr at that layer as:

$$T_{total} = \frac{P_r R_c}{(0.75) FS_{po}} \tag{2.12}$$

where Re is the coverage ratio and is often assumed to be unity for geotextiles and geomembranes. Pr is a function of embedment length Le, overburden stress, and coefficient of friction (or the friction bearing-interaction factor). According to the FHWA methodology, the coefficient of friction between the soil and reinforcement in the seismic condition should be reduced to 80% of the static value.

In evaluating the rupture failure during seismic loading, the reinforcement is to be designed to resist both the static and seismic forces, which requires the following:

$$T_{\max} \le \frac{S_{rs} . R_c}{(0.75) . RF_{CR} . RF_D . RF_{ID} . FS} \quad \text{(static component)} \tag{2.13}$$

$$T_{\max} \le \frac{S_{rt} . R_c}{(0.75) . RF_D . RF_{ID} . FS} \quad \text{(seismic component)} \tag{2.14}$$

where Rc = coverage ratio, RF_{CR}= creep reduction factor, RF_D = durability reduction factor, RF_{ID} = installation damage factor, FS = overall factor of safety, S_{rs} = reinforcement strength to resist static load, and S_{rt} = reinforcement strength to resist seismic load. Note that the creep reduction factor $RF_{CR}$is not applicable to Tmd, since seismic load occurs in a short time. The values of various reduction factors have been suggested in the FHWA methodology. Moreover, with both S_{rs} and S_{rt} known, the required ultimate strength of the geosynthetic reinforcement T_{ult} can be calculated as follows :

$$T_{ult} = S_{rs} + S_{rt} \tag{2.15}$$

A particular geosynthetic reinforcement can be selected based on the value of T_{ult}.

The connection pullout failure during seismic loading is evaluated using the following conditions:

$$T_{\max} \le \frac{S_{rs} . CR_c}{RF_D . FS} \tag{2.16}$$

$$T_{\max} \le 0.8\left(\frac{S_{rt}.CR_{ult}}{RF_D.FS}\right) \tag{2.17}$$

where CR_{cr} = connection strength reduction factor resulting from long-term testing and CR_{uit} = connection strength reduction factor resulting from quick connection tests. Both CR_{cr} and CR_{ult} are to be determined using the laboratory testing technique described in Appendix A of the FHWA manual. Both CR_{cr} and CR_{ult} are a function of normal stress, which is developed by the weight of the facing units. Calculation of normal stress should be limited by the hinge height in the case of a batter wall.

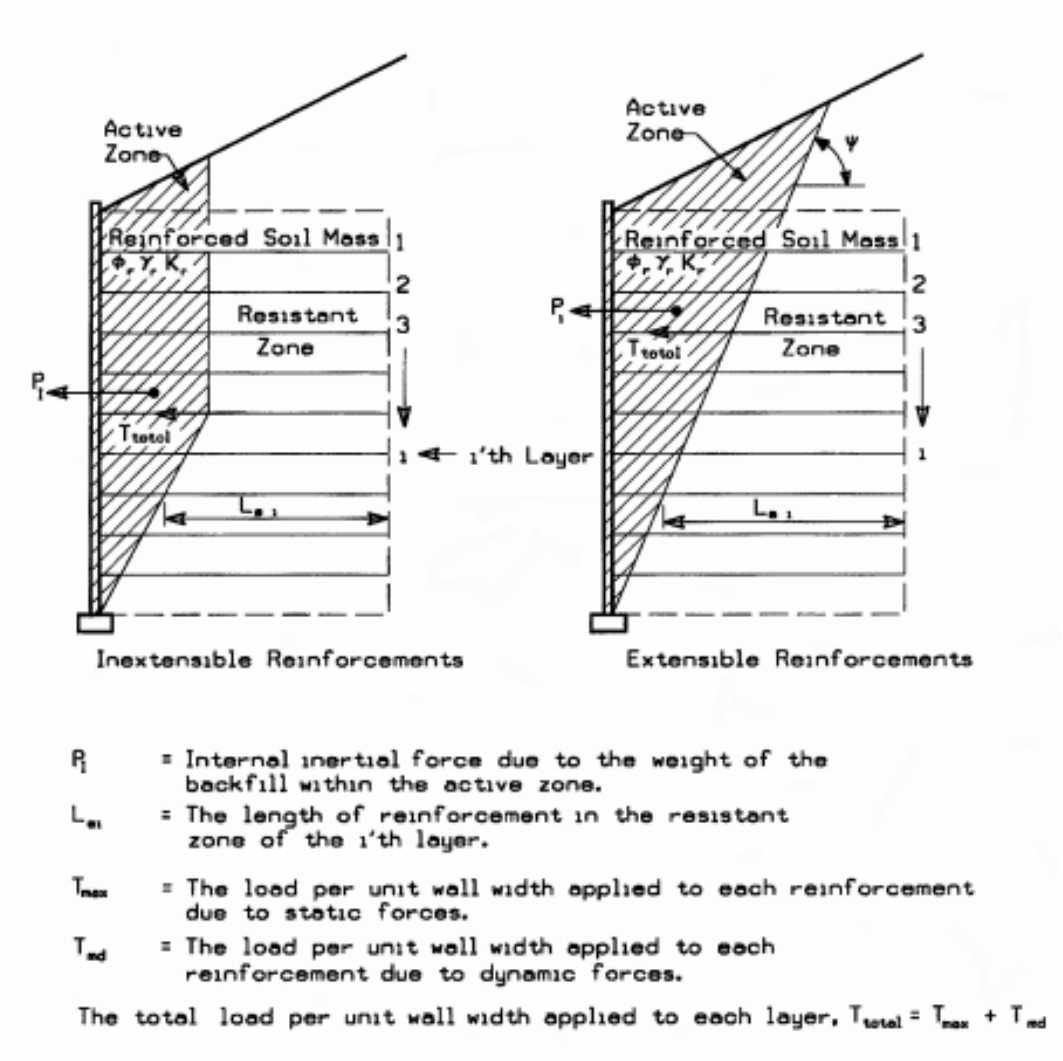

Figure 2.14 Seismic internal stability of a GRS wall in FHWA method.

2.4 Back-to-Back Retaining wall

Back-to-back walls are often used for highway ramps. For walls which are built back-to-back as shown in Figure 2.15, a modified value of lateral pressure influences the external stability calculations. As indicated in Figure 2.15, two cases can be considered and are discussed below.

Case I:

For Case I, the overall base width is large enough so that each wall behaves and can be designed independently. In particular, there is no overlapping of the reinforcements. Theoretically, if the distance, *D*, between the two walls is shorter than $D = H1 \tan(45° - \phi°/2)$ where H_1 is the taller of the parallel walls, then the active wedges at the back of each wall cannot fully spread out and the active thrust is reduced. However, for design it is assumed that for values of $D > H_1 \tan(45° - \phi°/2) \approx 0.5H_1$ then full active thrust is mobilized.

Case II:

For Case II, there is an overlapping of the reinforcements such that the two walls interact. When the overlap, L_R, is greater than $0.3H2$, where $H2$ is the shorter of the parallel walls, no active earth thrust from the backfill needs to be considered for external stability calculations. For intermediate geometries between Case I and Case II, the active earth thrust may be linearly interpolated from the full active case to zero.

For Case II geometries with overlaps (L_R) greater than $0.3H_2$, the following guidelines should be used:

- $L1/H1 \geq 0.6$ where $L1$ and $H1$ is the length of the reinforcement and height, respectively, of the taller wall.
- $L2/H2 \geq 0.6$ where $L2$ and $H2$ is the length of the reinforcement and height, respectively of the shorter wall.
- $Wb/H1 \geq 1.1$ where Wb is the base width as shown in Figure 2.15 and $H1$ is the height of the taller wall.

The above guidelines are valid for static load conditions or in areas where the seismic horizontal accelerations at the foundation level are less than 0.05g. Back-to-back walls in

seismically active areas should be designed based on a more detailed analysis that includes effects of potential non-uniform distribution of seismic and inertial forces within the wall.

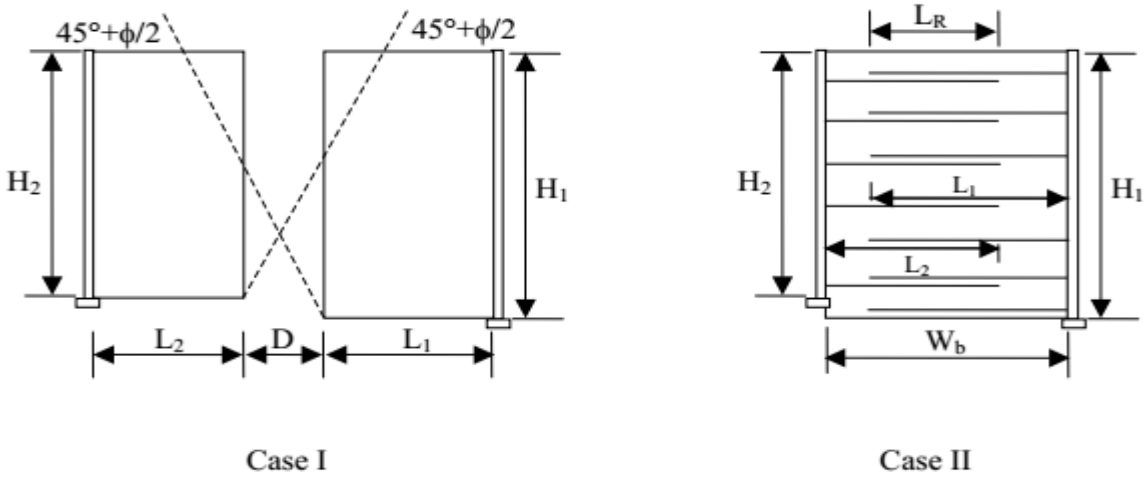

Figure 2.15 Back-to-back MSE walls.

Ling et al. (2003) had simulated an overpass in Turkey, using FLAG. Tensions in reinforcements and lateral displacements were computed for seismic loading. However, the model was basic which may simulate the exact field conditions. Hardianto and Truong (2010) had studied the effect of the aspect ratio of back-to-back walls on tensile forces under seismic loading. Lower aspect ratios were also analyzed using FLAC 6.00. However, the study was elementary as it did not consider the staged constriction and compaction stresses.

Han and Leshchisnskv 2010 studied back-to-back MSE retaining walls using FI.AC and ReSSA (limit-equilibrium-method based software). The effects of the ratio of the distance between the walls to the height of the walls (W/H ratio) and quality of backfill on the critical failure surface required the tensile strength of reinforcement, and lateral pressures at the end of the reinforced zone were analyzed. The analysis was performed at limit state condition using FI.AC. Limit equilibrium analysis was performed for only single walls and results were comparer! with the back-to-back walls. Walls of 6-m height were simulated. The angle of shearing resistance of the backfill(ϕ) of 25° and 34° and W/H ratio of 1.4, 2.0, and 3.0 were considered for the study. The critical failure surface was dictated to pass through the toe of the walls by providing the weaker bond strength at the bottom blocks of the facing. The shape and location of critical failure surfaces were analyzed for various W/H ratios and various angle of shearing resistance of the backfill. The critical failure surface of one wall interferes into the reinforced zone of the other wall in low W/H ratios. Figure 2.16 shows the interaction of critical

failure surfaces in W/H 1.4 and 2.0 for ϕ=25° and 34°. It was observed that the interference of failure extended to the greater depths as the angle of shearing resistance was decreased. In W\H=1.4, and ϕ=25°. the interaction between the failure surfaces extends up to about half the depth of the walls. As per FHVVA guidelines, for ϕ= 34°, walls with W/H= 2.0 should behave independently. However, the interaction of critical slip surfaces was observed for this configuration. In W\H=1.4, lateral force at the end of the reinforcement zone reduced to about 70% mid 85% of theoretical active Kankine lateral force in ϕ= 25°. and ϕ=34° respectively. The percentage reduction of lateral force with W\H ratio is more significant in ϕ=25° than ϕ=34°. The distribution of maximum tension in reinforcements with the depth of the wall in the unconnected walls was reported as linearly increasing up to a certain depth and then constant till the bottom of the wall. However, in connected walls maximum tension was constant all through the depth of the wall. A limit state, connected walls mobilize lesser tensions than that of unconnected walls. The value of maximum tension in reinforcement increases with a decrease in the angle of shearing resistance of the backfill. The maximum reinforcement tensions in walls with ϕ=25° were 67% and 100% higher than those of walls with ϕ=34° in connected and unconnected walls respectively. However, the model had not simulated staged construction and compaction stresses.

Anubhav and Basudhar (2011) studied the response of footing placed on a double-faced, wrap-around reinforced walls using numerical modeling in PLAXIS 2D. Authors have presented the influence of number of reinforcing layers and overlap length on load-deformation behavior, the ultimate bearing capacity of footing, and lateral deformations. The numerical results were validated using experimental data. Experiments were conducted in a small-scale tank. The numerical model could predict the experimental data with minimum error. However, the numerical and experimental model was simulated a wall of height 0.5m and the results might be affected with full-scale wall.

Katkar and Viswanadham (2011) analyzed back-to-back walls using finite element. software-PLAXIS 2D. t he study aimed in examining the effect of distance between the ends of the reinforcements of the walls (D) and angle of shearing resistance of backfill on the lateral displacements and maximum tensions in the reinforcements. A wall of 6-m height was considered. Four cases were considered with different D/H ratios ranging from 0 to 1.6. The connection of reinforcements was also studied. Lateral displacements and the maximum tension in the reinforcements were studied. Lateral displacements reduced drastically in the case of

connected reinforcements. However, the maximum tension in the reinforcement in the connected case was found to be higher than that for the unconnected case. However, the model was a basic model which did not consider staged construction.

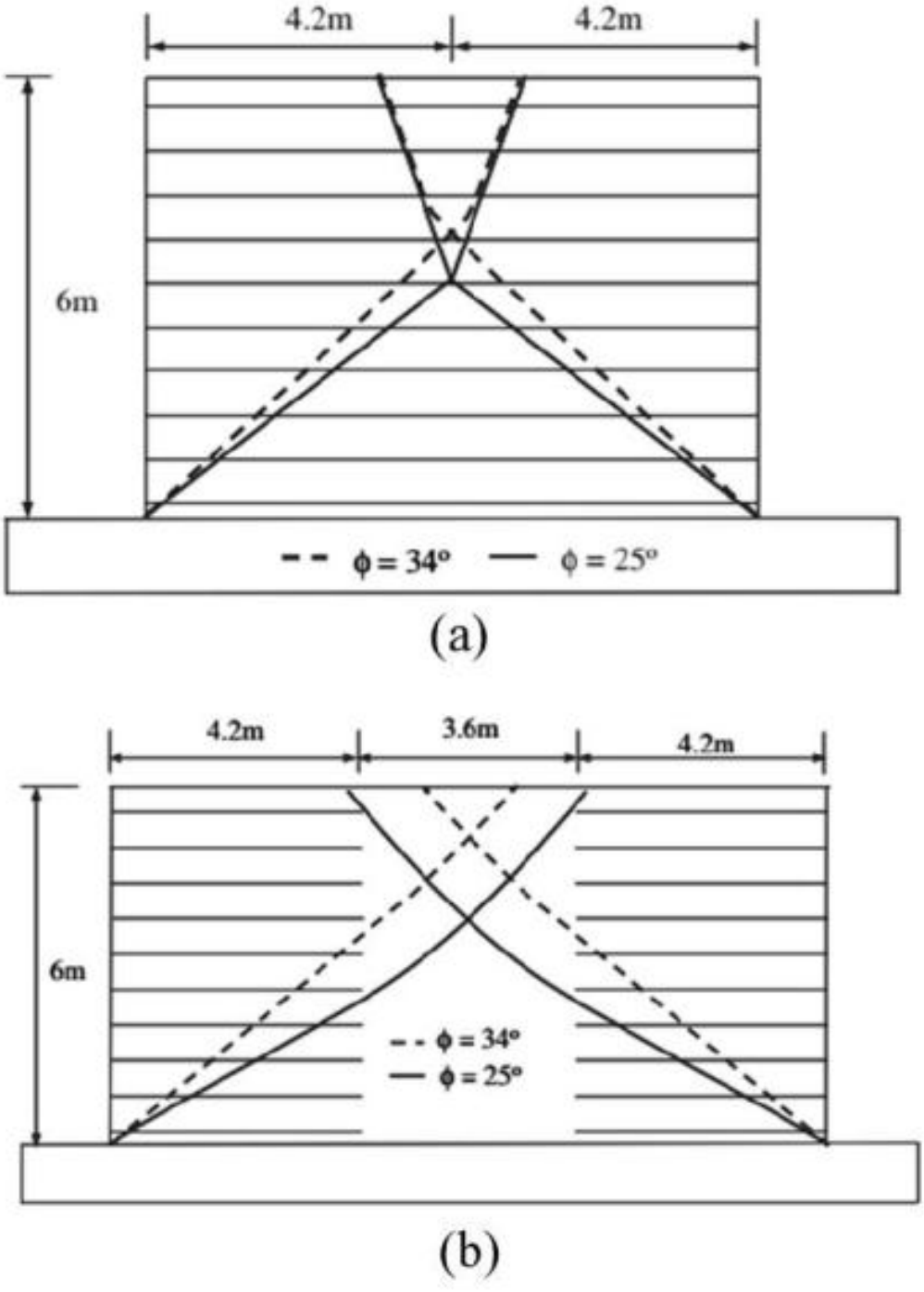

Figure 2.16 Influence of angle of shearing resistance of backfill on ceitical failure surface in back-to back walls in (a) W/H=1.4 and (b) W/H= 2.

Katkar and Viswanadham (2012) conducted centrifuge model tests to study the behavior of single vertical wall, and back-to-back geogrid reinforced walls constructed using the wrap-around technique. The effect of reinforcement connection in the middle of the wall was also analyzed. In this study, three cases were considered. Single reinforced wall, back-to-back walls with unconnected reinforcement, and back-to-back walls with reinforcement connected in the middle were considered. Lateral deformations, strains in the reinforcements, and surface settlements were studied. Loading was given from 10g to 60g. It was found that the connected walls had lesser lateral deformations than those of unconnected walls. However, the peak strains in the reinforcements were highest in the connected walls at 45g.

El-Sherbiny et al. (2013) used the finite element method (PLAXIS) to simulate a back-to-back walls model. Effect of distance between the walls on the lateral pressures, lateral displacements, and the maximum tensions in the reinforcement was studied under working-stress condition. The formation of the critical slip surface and overall factor of safety of the back-to-back walls were analyzed under limit-state condition. It was found that as the distance between the walls decreases from 0.5H to zero, the lateral earth pressures decreases by approximately 25% and the maximum tensile force in the reinforcement reduces by 5%. -10%. The length of reinforcement was also varied to investigate the effect in reducing the length to less than 0.7H. The reduction in the length of reinforcement increased the horizontal deformation and the maximum tensile forces. However, the study did not mention about the interfaces used and the study did not consider the compaction stresses.

Benmebarek et al. (2016) modeled back-to-back walls incorporating staged construction using Finite Element Program (PLAXIS). Critical failure surfaces, lateral pressures at the end of the reinforcement zone, lateral displacements and maximum tension profile along the height of the wall were investigated for various W/H ratios. The study concluded that interaction between the walls exist even when the W/H ratio is more than 2 for an internal angle of shearing resistance of backfill of 35° (as per FHWA guidelines, both the walls should behave independently for W/H > = 1.93). W/H ratio had a significant influence on the lateral pressures at the end of the reinforcement zone. Influence of cohesion in the backfill material was also analyzed. A small reduction in the lateral pressures was observed.

Djabri and Benmebarek (2016) analyzed back-to-back walls using limit state approach. Effect of W/H ratio on the lateral earth pressures, maximum tension profiles and critical failure surface was dealt. Djabri and Benmebarek (2016) analyzed W/H ratio effect on lateral displacements and the maximum tension line. In both the above studies, the effect of reinforcement stiffness was not considered. Model did not consider the surcharge loads also.

Benmebarek and Djabri (2017a) investigated the effect of overlap length in the back-to-back walls using PL AXIS. The influence of overlapping length on the factor of safety, lateral displacements, maximum tension in the reinforcement, potential failure surface for internal stability was studied. It is found that the factor of safety was increasing by 50% with an increase in overlapping length from 0.1 LR/H to 0.4 LR/H. Lateral displacements decreased by more than 20% when overlapping length increases. Reinforcement tension had minimal effect with the overlap length. The effect of the height of the walls was also studied. However, the interface between the facing panel was simulated as hinges which might not simulate the exact interaction of the facing panels.

Benmebarek and Djabri (2017b) investigated for simple cyclic harmonic loading in back-to-back MSG walls. It concluded that the lateral deformations and maximum tensile force in the reinforcements were affected by the variation of W/H ratios in this loading condition. When the W/H ratio is decreased, the amplitude displacement decreases drastically. The stability of back-to-back walls significantly depended on peak ground acceleration and frequency of loading. The study concluded that lateral displacements and maximum reinforcement tension forces were not linearly related to the characteristics of loading. However, a detailed study in back-to-back walls with respect to the compaction stresses and surcharge loads was required. The reinforcement stiffness effect was not studied in any of the above studies.

Dram (2021) investigated the dynamic response of connected and unconnected back-to-back mechanically stabilized earth walls under earthquake loading using the finite element method. The total seismic earth thrusts at the end of the reinforced zone and at the facing of BBMSE walls and their points of application were presented (refer Figure 2.17).

Brouthen (2022) conducted FE analysis by using PLAXIS 2D software to investigate the behaviour of problem geometry, strip pre-tensioning, strip type, and surcharging on horizontal displacements, development of soil shear and plastic zones, lateral earth pressure, and reinforcement loads is presented. The results of this study found that reduced by about 30% due to the improved polymeric–soil interface strength and stiffness. The results of this study

revealed a reduction of approximately 30% due to improved polymeric–soil interface strength and stiffness, as shown in Figure 2.18.

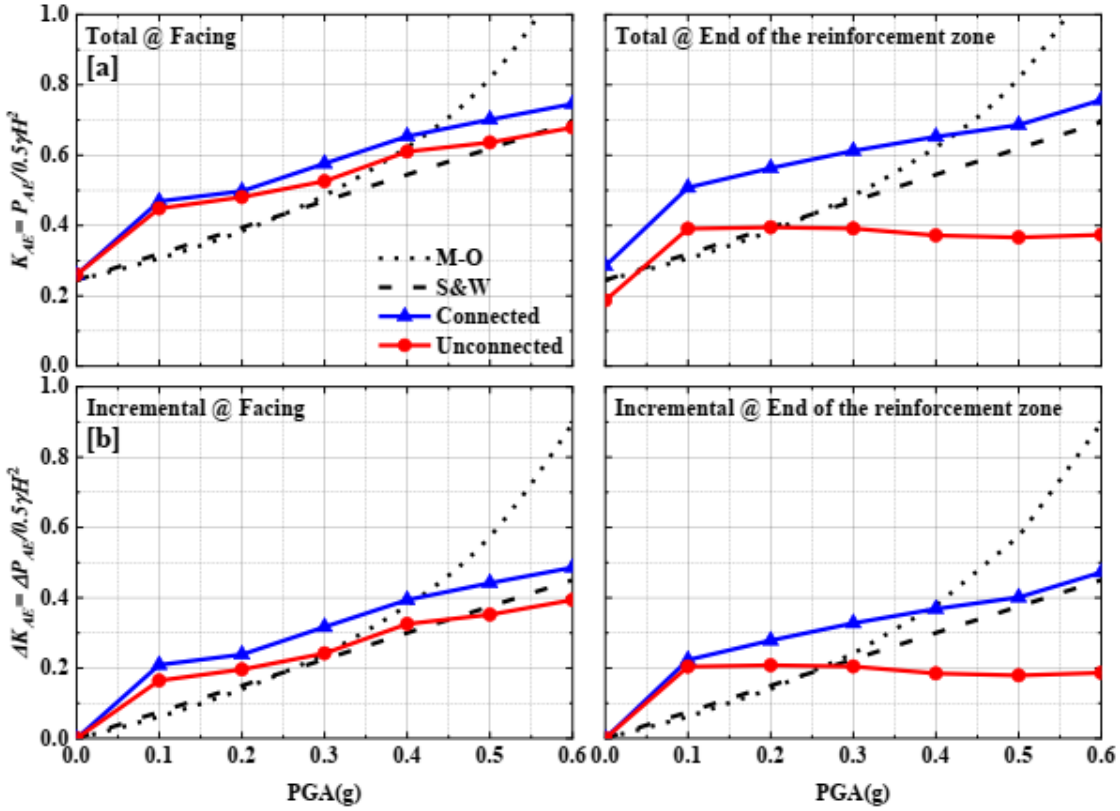

.

Figure 2.17 Variations in normalized total earth pressures at facing and end of reinforcement zone of connected and unconnected walls showing (a) total ,and (b) incremental values.

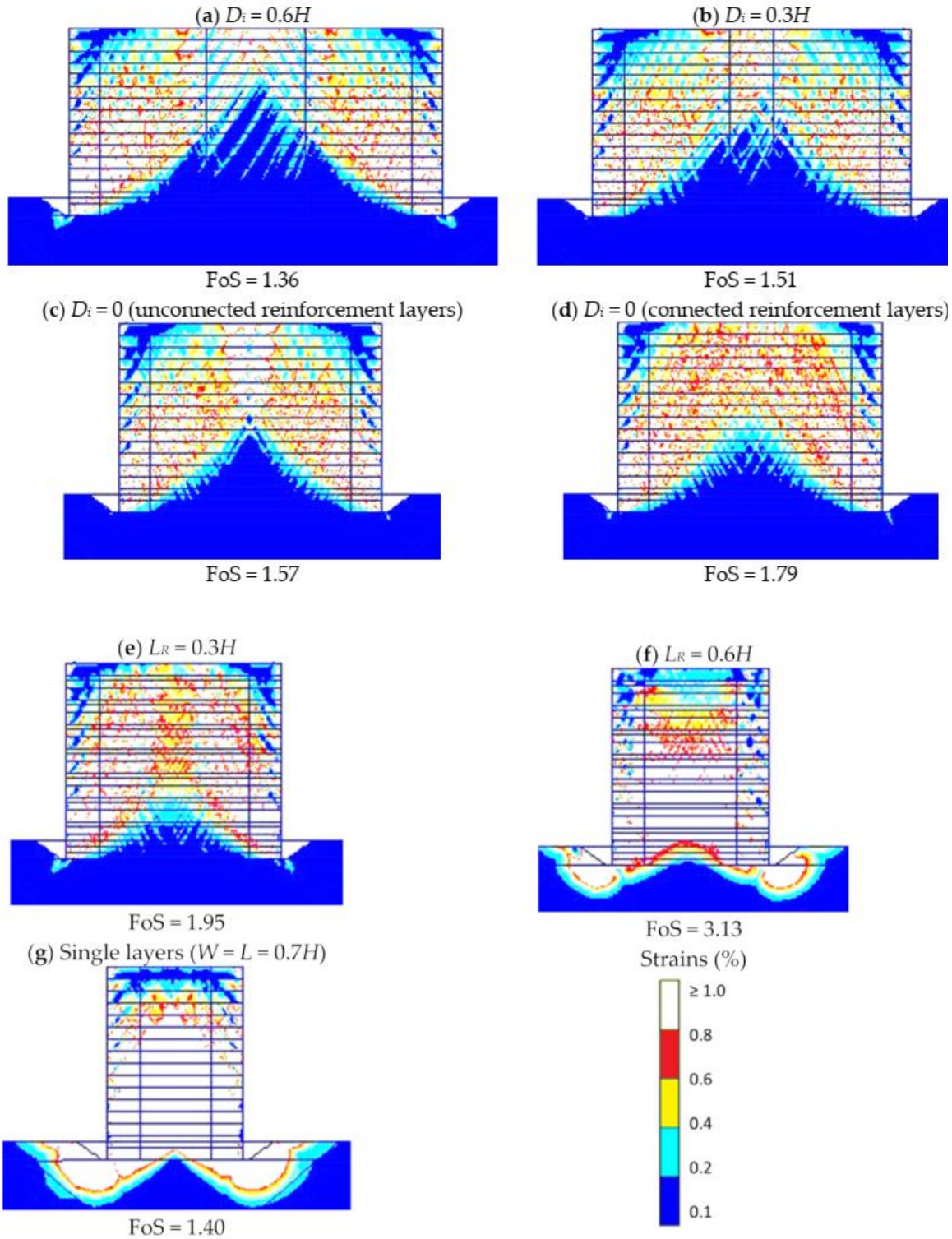

Figure 2.18 Shear strain contours at failure with the c- reduction at end of construction (EoC) for walls with different interaction distances(D_i)between the back of the reinforced soil zones for opposite walls. Note: results range from 0-1%.

2.5 Conclusions

In this Chapter, a review of the single wall studies was dealt. A review of analytical, numerical, and experimental methods proposed to investigate the seismic response of a reinforced retaining wall was presented. A review on compaction stress and surcharge was presented. The literature on back-to-back walls for different parameters like reinforcement stiffness, types of wall facia, battered angle of the facia was limited. Hence, an extensive study on back-to-back walls is needed to study the intricacies of the problem. A brief introduction the MSE wall design procedures that is available in the literature was also presented.

SECOND PART

NUMERICAL MODELING

Chapter 3

Analysis of Back-to-Back Reinforced Retaining Walls with Panel Facia

3.1 Introduction

This chapter, describes the results of the stability of embankment bridge approaches constructed by close back-to-back geosynthetic reinforced soil retaining walls self-weight. A numerical model was developed to analyze the maximum displacements; the tensile forces mobilized in geogrid layers and the lateral earth pressure of MSE walls. The numerical results show how this type of reinforced soil walls perform jointly at a certain distance of interaction between the two opposite walls.

3.2 Finite Element Modeling

In the present study, a finite element-based program, PLAXIS 2D, was used to develop a plane-strain model to analysis of the MSE walls. A 6 m-high wall resting on a 2 m-thick soil foundation was considered. Figures 3.1, 3.2, 3.3, and 3.4 represents a finite element model of back-to-back MSE walls. For this, a basic model is chosen with three different ratios of L_R/H = 0; 0.3 and 0.6, the length of the reinforcements for the two walls was considered as L = 4.2 m (the typical rebar length recommended by FHWA design guidelines (FHWA 2009), i.e. $L=0.7H$).

3.2.1 Soil Proprieties

The foundation soil was modeled as Mohr-Coulomb material with very high deformation modulus (E=200 MPa) to simulate it as a rigid material. The model involves six input parameters, namely, deformation modulus (E), Poisson ratio (ν), cohesion (c), friction angle (φ), and dilatancy angle (ψ). Table 3.1 presents the values of the material properties considered in the study. The soil-reinforcement interaction was modeled by relating the nonlinear elastic behavior of the soil to the linear elastic response of the reinforcement. For this purpose, the geogrids are selected from the

elastoplastic elements with stiffness and tensile strength. The interaction between the geogrid and soil was simulated using interface element.

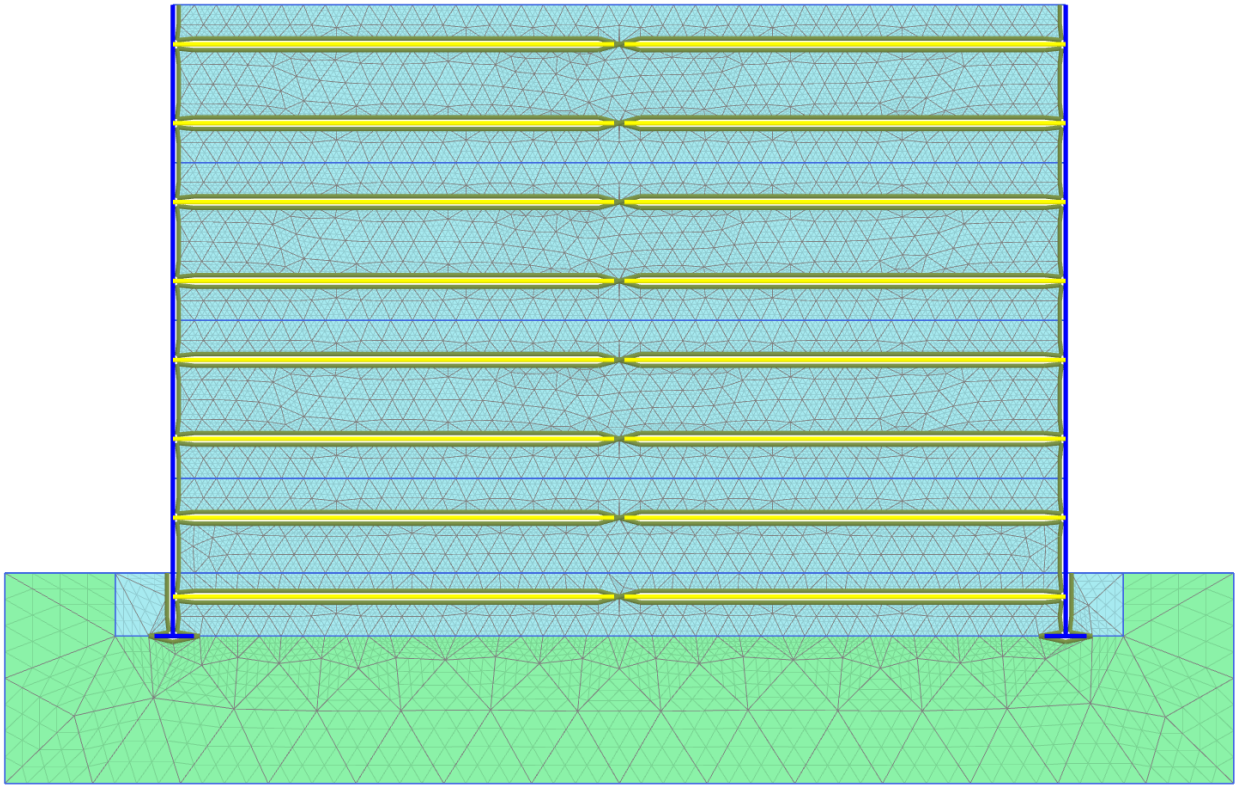

Figure 3.1 Finite element models of back-to-back MSE walls.

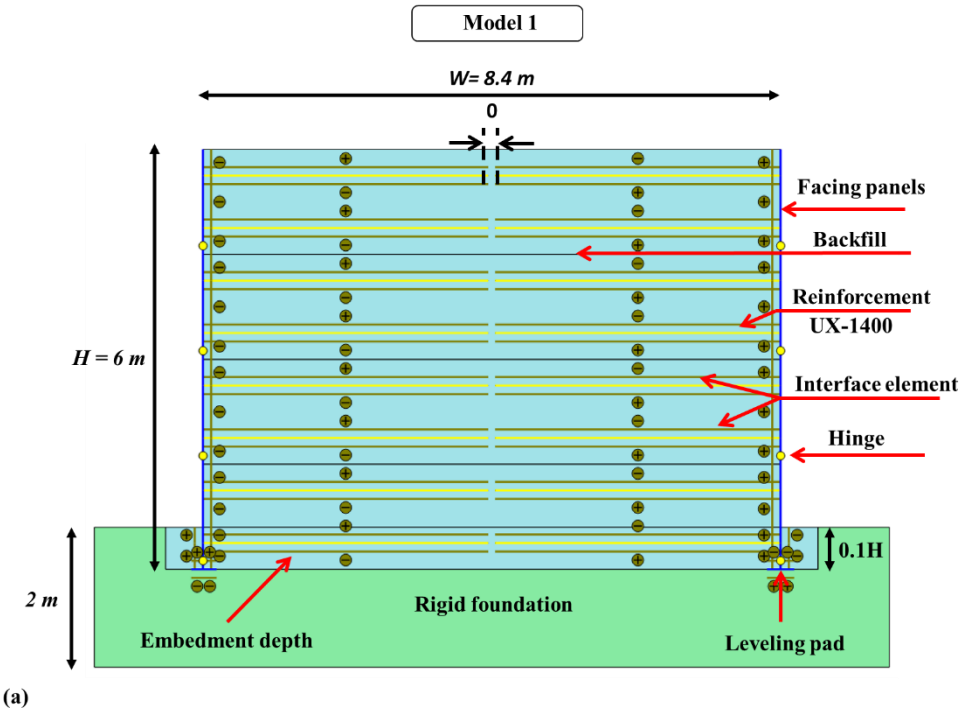

Figure 3.1 Finite element models of back-to-back MSE walls (*Overlap length L_R=0*).

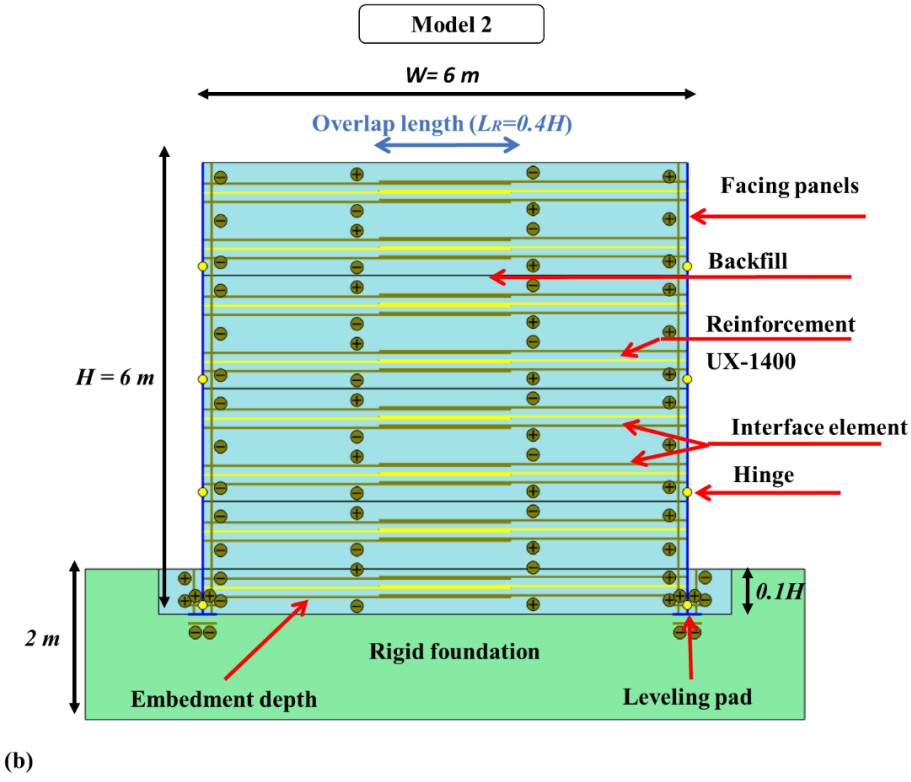

Figure 3.1 Finite element models of back-to-back MSE walls (*Overlap length L_R=0.4H*).

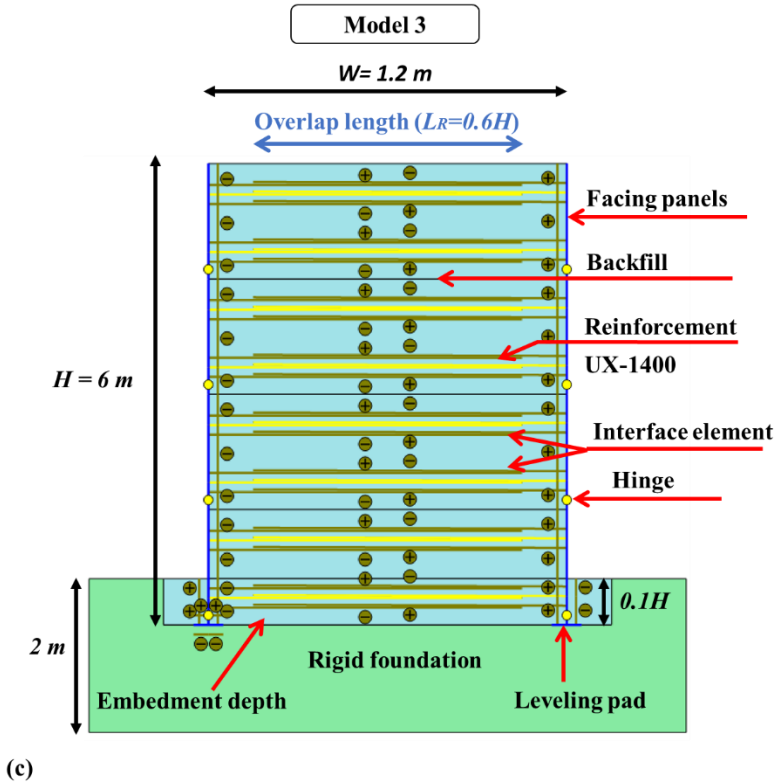

Figure 3.1 Finite element models of back-to-back MSE walls (*Overlap length L_R=0.6H*).

Table 3. 1. Material properties used in numerical simulations.

Material	Symbol	Unit	Reinforced backfill	Foundation soil
Unit weight	γ_s	kN/m^3	18	22
Angle of shearing resistance	ϕ	degrees	35	30
Dilatancy angle	ψ	degrees	5	0
Deformation modulus	E	kPa	30×10^3	200×10^3
Cohesion	c	kPa	0	200
Poisson's ratio	v	-	0.3	0.2

Table3. 2. Reinforcement properties.

Identification	Model	Ultimate tensile strength	Allowable tensile strength, T_a	Axial stiffness
Uniaxial geogrid	Elastoplastic	70 kN/m	25.6 kN/m	1,100 kN/m

3.2.2 Reinforcement

Table 3.2 gives the properties of the reinforcement - uniaxial geogrid (UX-1400 type). Geogrids were placed at typical pacing of 0.75 m (AASTHO 2012). The well-known segmental precast concrete panels were considered in the current study to simulate the wall. Each wall contains 4 segmental concrete panels of 1.5 m in width and height and 0.14 m in thickness.

3.2.3 Facing: Precast Panels

The concrete panel facia was modeled as a linear-elastic material. In the present model, the facing panel was hinged to a horizontal plate which is 0.5m embedded in the foundation soil. Hence the panel had the flexibility to move in horizontal direction. However, the panel cannot be moved in vertical direction. The boundary condition applied in the model, simulates the real situation of embedment with nominal footing at the bottom of the concrete panel. Hence, nominal lateral displacements can be expected in the real time scenario for the seismic loading. In the finite element model, the properties of the facing panel were defined by its Young's modulus, E = 25 GPa and the unit weight γ_c= 23.5 kN/m^3. Table 3.3 gives the properties of the facia considered in the study.

Table 3. 3. Material properties of concrete panel facing elements.

Identification	Elastic stiffness (*EA*)	Flexural rigidity (*EI*)	Thickness (*d*)	Weight of panel (W_c)	Poisson ratio (v_c)
Concrete panel facia	3.5×10^6 kN/m	5,717 kN/m^2 /m	0.14 m	3.29 kN/m/m	0.2

3.2.4 Interface properties

The interaction between the facing panel elements and the backfill and between the backfill and reinforcement were modeled by using interface elements (refer to Figure 3.1). A partially rough interface was considered, such that the interface parameter, R_{inter}, was equal to $\tan \delta' / \tan \varphi$, where interface friction angle $\delta' = 23.0°$ and backfill friction angle $\varphi = 35°$. For the present study, the interface strength was reduced by using the strength reduction factor = 0.60 < 1 in these analyses.

3.4 Results and Discussions

3.4.1 Lateral displacements of the wall

Figure 3.2 shows the variations of the maximum normalized displacements at the facing for different back-to-back MSE walls (BBMSEWs), overlapping length reinforcement distances (L_R). The results suggest that connecting the walls on both sides of BBMSEWs reduces lateral displacements significantly. Separating two opposed walls from one other, on the other hand, causes a local increase in lateral displacement profile. This local increase is clearly seen in lateral displacement profile of Model 1. As shown in Fig. 6, using L_R = 0.4H in Model 2 reduces maximum horizontal movements by about 21%, while increasing L_R = 0.6H reduces maximum horizontal displacements by around 19% percent (Models 3), as compared to Model 1.

3.4.2 Lateral earth pressures behind wall.

Figure 3.3 depicts the normalized lateral earth pressure behind the wall, the lateral earth pressure was normalized with respect to γH. Accordingly, the earth pressures from the numerical model were presented and compared with those the active Rankine. However, the lateral earth pressure decreases as the overlapping L_R increases from 0.4H to 0.6H when compared with that of the Model 1 ($L_R = 0$).

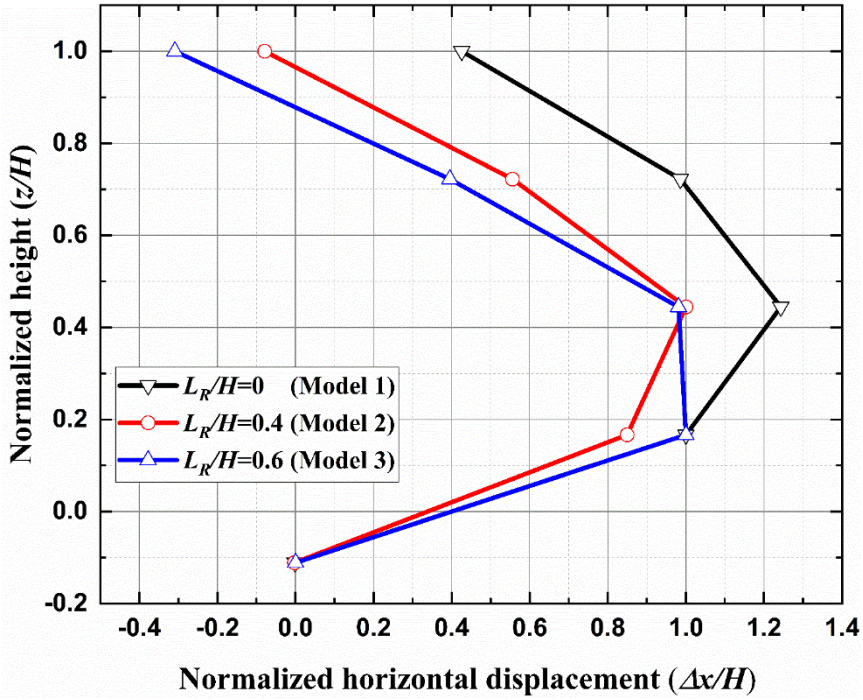

Figure 3.2 Horizontal wall displacements for the L_R/H = 0; 0.4 and 0.6.

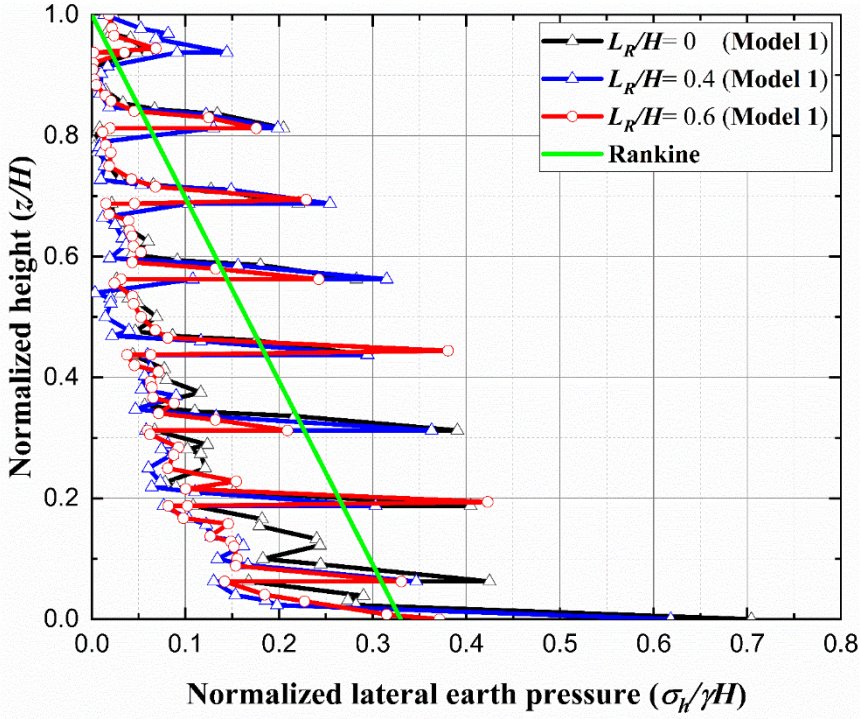

Figure 3.3 Lateral earth pressure at the facing for the L_R/H = 0; 0.4 and 0.6

3.4.3 Distribution of tensile force in reinforcements

Figure 3.4 shows the maximum tensile forces in the geogrid layers were normalized with the product of soil unit weight (γ), the geogrid vertical intervals (S_V) and the wall height (H). The results indicate that the bottom reinforcements experience the maximum force compared to those of the top reinforcements of the facing. As expected from previous results, the high tensile force in the reinforcements the base of the wall was the result of both high overburden stress and a retaining effect due to geogrid reinforcements. As expected from previous results, the tensile loads become less with decreasing interaction distance the overlapping L_R.

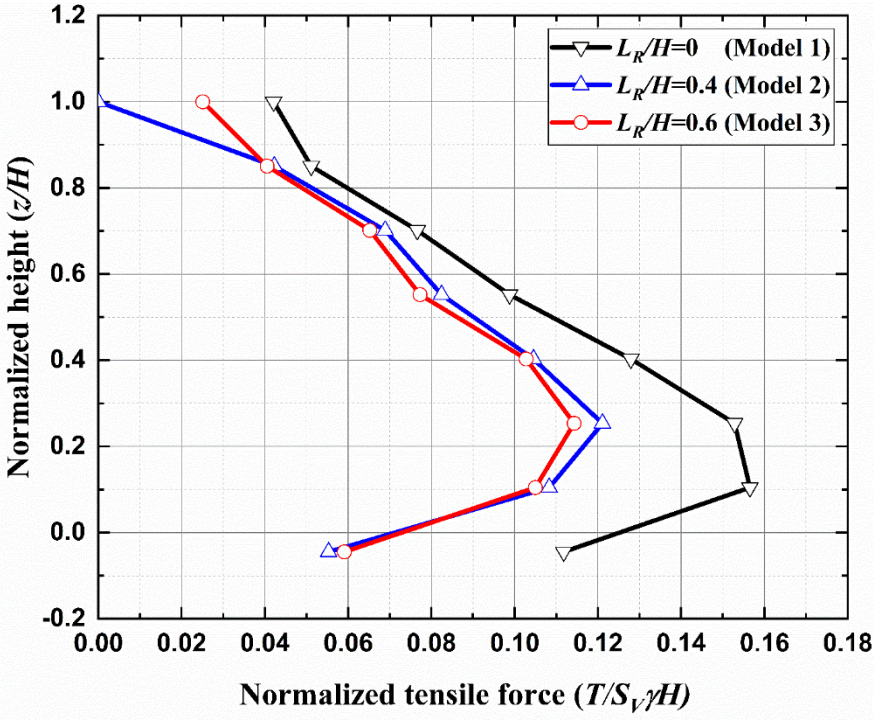

Figure 3.4 Distribution of maximum tension in reinforcement.

3.5 Conclusions

The findings revealed that entirely linking two opposing walls to each other, can significantly reduce BBMSEW lateral displacements. Separating two walls from each other locally causes a local rise in the lateral displacement profile, and complete separation of walls from each other causes the lateral displacements to reach their maximum value, making this sort of reinforcing arrangement the most inappropriate for BBMSEWs.

GENERAL SUMMARY

The effect of using geogrids to reinforce bridge abutments and retaining walls is a complicated phenomenon that limits the use of analytical computations. Professional tools (such as ABACUS, FLAC, PLAXIS, etc.) are required for numerical modeling of this effect, which includes reinforcement elements, interface elements, and elasto-plastic behavior models. With a Mohr-Coulomb type criterion, models of elasto-plastic behavior can be created.
Bridge abutments, piled walls, and double-faced (or opposing) walls are examples of complicated geometric constructions. The latter are frequently used to build bridge access embankments to raise heights. As a result, they were the focus of our thesis contribution.

The first part's bibliographical analysis allowed us to highlight information about the behavior of conventional retaining walls in reinforced soil. This information is extremely important in this study and will continue to be useful in the future.
In the second part, we ran three numerical simulations of bridge access embankment behavior. The construction is made up of double-faced (back-to-back) retaining walls constructed of soils that are strengthened with geosynthetics.

The analysis of the simulation results by PLAXIS of the applications allowed us to conclude:

- The reduction of the reinforcement overlap length induces an increase of the maximum horizontal displacement. Thus, the classical theoretical calculation becomes too backward, so the effect of overlapping reinforcements must be taken into account for the dimensioning of the external stability of bridge access embankments.

- The internal stability is unaffected by the reinforcement overlap. As a result, a traditional method of calculating the internal stability of a single-sided retaining wall can be utilized to build the joint walls that make up the bridge access embankment.

- In some cases, overlapping reinforcements will lower the length of reinforcement to 0.4H, which is less than the 0.6H recommended by the 2009 FHWA guidelines.

Finally, due to their geometry and the extensibility of the synthetic reinforcements, the modeling of abutments built of soil reinforced with synthetic reinforcements displays a more complex behavior, which limits the analytical calculations. Unfortunately, experimental evidence on real or full-scale structures is insufficient for a complete understanding of this type of structure, and numerical modeling appears to be nearly non-existent. However, it appears that ensuring the continuity of this work is beneficial.

BIBLIOGRAPHIC REFERENCES

AASTHO. 2012. AASHTO LRFD Bridge design specifications, 6th edn. American Association of State Highway and Transportation Officials (AASHTO), Washington DC.

Anubhav, S., & Basudhar, P. (2011). Numerical modelling of surface strip footings resting on double-faced wrap-around vertical reinforced soil walls. Geosynthetics International, 18(1), 21-34.

Alhajj Chehade, H. (2021). *Geosynthetic-reinforced retaining walls-Deterministic and Probabilistic Approaches* (Doctoral dissertation, Université Grenoble Alpes).

Bathurst, R. J., & Hatami, K. (1998). Seismic response analysis of a geosynthetic-reinforced soil retaining wall. Geosynthetics International, 5(1-2), 127-166.

Berg, R. R., Christopher, B. R., & Samtani, N. C. (2009). Design of mechanically stabilized earth walls and reinforced soil slopes–Volume I: United States. Federal Highway Administration.

Benmebarek, S., Attallaoui, S., & Benmebarek, N. (2016). Interaction analysis of back-to-back mechanically stabilized earth walls. Journal of Rock Mechanics and Geotechnical Engineering, 8(5), 697-702.

Benmebarek, S., & Djabri, M. (2017a). FE Analysis of Back-to-Back Mechanically Stabilized Earth Walls Under Cyclic Harmonic Loading. Indian Geotechnical Journal.

Benmebarek, S., & Djabri, M. (2017b). FEM to investigate the effect of overlapping-reinforcement on the performance of back-to-back embankment bridge approaches under self-weight. Transportation Geotechnics, 11, 17-26.

Brouthen, A., Houhou, M. N., & Damians, I. P. (2022). Numerical Study of the Influence of the Interaction Distance, the Polymeric Strips Pre-Tensioning, and the Soil–Polymeric Interaction on the Performance of Back-to-Back Reinforced Soil Walls. Infrastructures, 7(2), 22.

Bhuiyan, M. Z. I. (2012). *Interface shear capacity of facing units of geosynthetic-reinforced segmental retaining walls* (Doctoral dissertation, Jabatan Kejuteraan Awam, Fakulti Kejuruteraan, Universiti Malaya).

Dram, A., Balunaini, U., Benmebarek, S., Sravanam, S. M., & Madhav, M. R. (2021). Earthquake response of connected and unconnected back-to-back geosynthetic-reinforced soil walls. International Journal of Geomechanics, 21(11), 04021223.

Djabri, M., & Benmebarek, S. (2016). FEM Analysis of Back-to-Back Geosynthetic-Reinforced Soil Retaining Walls. International Journal of Geosynthetics and Ground Engineering, 2(3).

Djabri, M., & Benmebarek, S. (2020). Numerical Investigations on the Behavior of Back-to-Back Mechanically Stabilized Earth Walls: Effect of Structural Components. Jordan Journal of Civil Engineering, 14(3).

Cai, Z., & Bathurst, R. J. (1995). Seismic response analysis of geosynthetic reinforced soil segmental retaining walls by finite element method. Computers and Geotechnics, 17(4), 523-546.

Chida, S., Minami, K., & Adachi, K. (1985). Tests with regard to the stability of the fill constructed by the reinforced earth technique. unpublished report translated from Japanese.

El-Emam, M. M., & Bathurst, R. J. (2007). Influence of reinforcement parameters on the seismic response of reduced-scale reinforced soil retaining walls. Geotextiles and Geomembranes, 25(1), 33-49.

El-Emam, M. M., & Bathurst, R. J. (2005). Facing contribution to seismic response of reduced-scale reinforced soil walls. Geosynthetics International, 12(5), 215-238.

El-Sherbiny, R., Ibrahim, E., & Salem, A. (2013). Stability of back-to-back mechanically stabilized earth walls. Paper presented at the Geo-Congress 2013: Stability and Performance of Slopes and Embankments III.

Elias, V., Christopher, B. R., Berg, R. R., & Berg, R. R. (2001). Mechanically stabilized earth walls and reinforced soil slopes: design and construction guidelines (updated version) (No. FHWA-NHI-00-043). United States. Federal Highway Administration.

Fakharian, K., & Attar, I. H. (2007). Static and seismic numerical modeling of geosynthetic-reinforced soil segmental bridge abutments. Geosynthetics International, 14(4), 228-243.

Hatami, K., & Bathurst, R. J. (2000a). Effect of structural design on fundamental frequency of reinforced-soil retaining walls. Soil Dynamics and Earthquake Engineering, 19(3), 137-157.

Hatami, K., & Bathurst, R. J. (2001). Investigation of seismic response of reinforced soil retaining walls.

Helwany, M. B., & McCallen, D. (2001). Seismic analysis of segmental retaining walls. II: Effects of facing details. Journal of geotechnical and geoenvironmental engineering, 127(9), 750-756.

Hardianto, F. S., and K. M. Truong. (2010). Seismic deformation of back-to-back mechanically stabilized earth (MSE) walls. In Earth Retent. Conf. 3, Geotechnical Special Publication 208, edited by R. Finno, Y. M. A. Hashash, and P. Arduino, 704–711. Bellevue, WA: ASCE.

Han, J., and D. Leshchinsky. (2010). Analysis of back-to-back mechanically stabilized earth walls. Geotext. Geomembr. 28 (3): 262–267.

Koseki, J., Munaf, Y., Sato, T., Tatsuoka, F., Tateyama, M., & Kojima, K. (1998). Shaking and tilt table tests of geosynthetic-reinforced soil and conventional-type retaining walls. Geosynthetics International, 5(1-2), 73-96.

Koseki, J., Bathurst, R. J., Guler, E., Kuwano, J., & Maugeri, M. (2006, September). Seismic stability of reinforced soil walls. In 8th international conference on geosynthetics (Vol. 1, pp. 51-78).

Katkar, B. H., & Viswanadham, B. V. S. (2011). SOME STUDIES ON THE BEHAVIOUR OF BACK-TO-BACK GEOSYNTHETIC REINFORCED SOIL WALLS. In Proceedings of Indian Geotechnical Conference (IGC 2011) (Vol. 15).

Richardson, G. N., & Lee, K. L. (1975). Seismic design of reinforced earth walls. Journal of the geotechnical engineering division, 101(2), 167-188.

Sakaguchi, M. (1996). A study of the seismic behavior of geosynthetic reinforced walls in Japan. Geosynthetics International, 3(1), 13-30.

Siddharthan, R. V., Ganeshwara, V., Kutter, B. L., El-Desouky, M., & Whitman, R. V. (2004). Seismic deformation of bar mat mechanically stabilized earth walls. I: Centrifuge tests. Journal of geotechnical and geoenvironmental engineering, 130(1), 14-25.

Segrestin, P., & Bastick, M. J. (1988). Seismic design of reinforced earth retaining walls-the contribution of finiteelements analysis. In International geotechnical symposium on theory and practice of earth reinforcement (pp. 577-582).

Transportation Officials. (2002). Standard specifications for highway bridges. Aashto.

Takemura, J., & Takahashi, A. (2003). Centrifuge modeling of seismic performance of reinforced earth structures. In Reinforced soil engineering (pp. 414-438). CRC Press.

Leblanc, K. P. (2002). Performance of two full-scale geosynthetic reinforced segmental retaining walls. M.S. Thesis, Royal Military college of Canada (RMC), Kingston, Ontario, Canada.

Ling, H. I., Liu, H., Kaliakin, V. N., & Leshchinsky, D. (2004). Analyzing dynamic behavior of geosynthetic-reinforced soil retaining walls. Journal of Engineering Mechanics, 130(8), 911.

Ling, H. I., Mohri, Y., Leshchinsky, D., Burke, C., Matsushima, K., & Liu, H. (2005a). Large-scale shaking table tests on modular-block reinforced soil retaining walls. Journal of Geotechnical and Geoenvironmental Engineering, 131(4), 465-476.

Ling, H. I., Liu, H., & Mohri, Y. (2005b). Parametric studies on the behavior of reinforced soil retaining walls under earthquake loading. Journal of engineering mechanics, 131(10), 1056-1065.

Ling, H. I., Yang, S., Leshchinsky, D., Liu, H., & Burke, C. (2010). Finite-element simulations of full-scale modular-block reinforced soil retaining walls under earthquake loading. Journal of engineering mechanics, 136(5), 653-661.

Ling, H. I., & Leshchinsky, D. (2003). Finite element parametric study of the behavior of segmental block reinforced-soil retaining walls. Geosynthetics International, 10(3), 77-94.

Liu, H., Wang, X., & Song, E. (2010). Centrifuge testing of segmental geosynthetic-reinforced soil retaining walls subject to modest seismic loading. In GeoFlorida 2010: Advances in Analysis, Modeling & Design (pp. 2992-2998).

Lee, K. Z. Z., Chang, N. Y., & Ko, H. Y. (2010). Numerical simulation of geosynthetic-reinforced soil walls under seismic shaking. Geotextiles and Geomembranes, 28(4), 317-334.

Lee, K. Z. Z., & Chang, N. Y. (2012). Predictive modeling on seismic performances of geosynthetic-reinforced soil walls. Geotextiles and Geomembranes, 35, 25-40.

Lee, Z. Z. (2011). Geosynthetic-reinforced soil walls under multidirectional seismic shaking. University of Colorado at Denver.

Murali Krishna, A., & Madhavi Latha, G. (2007). Seismic response of wrap-faced reinforced soil-retaining wall models using shaking table tests. Geosynthetics International, 14(6), 355-364.

Murali Krishna, A., & Madhavi Latha, G. (2009). Seismic behaviour of rigid-faced reinforced soil retaining wall models: reinforcement effect. Geosynthetics International, 16(5), 364-373.

Matsuo, O., Yokoyama, K., & Saito, Y. (1998). Shaking table tests and analyses of geosynthetic-reinforced soil retaining walls. Geosynthetics International, 5(1-2), 97-126.

Nova-Roessig, L., & Sitar, N. (2006). Centrifuge model studies of the seismic response of reinforced soil slopes. Journal of Geotechnical and Geoenvironmental Engineering, 132(3), 388-400.

Yogendrakumar, M., & Bathurst, R. J. (1992). Numerical simulation of reinforced soil structures during blast loads. Transportation research record, 1336(1), 8.

Yogendrakumar, M., Bathurst, R. J., & Finn, W. L. (1992). Dynamic response analysis of reinforced-soil retaining wall. Journal of geotechnical engineering, 118(8), 1158-1167.